(19) Europäisches Patentamt
European Patent Office
Office européen des brevets

(11) Publication number: **0 299 498 A1**

(12) EUROPEAN PATENT APPLICATION

(21) Application number: 88111364.1

(51) Int. Cl.⁴: H01F 27/24

(22) Date of filing: 14.07.88

(30) Priority: 14.07.87 JP 175673/87
28.07.87 JP 188344/87
28.07.87 JP 188345/87
07.01.88 JP 1731/88

(43) Date of publication of application:
18.01.89 Bulletin 89/03

(84) Designated Contracting States:
DE FR GB

(71) Applicant: HITACHI METALS, LTD.
1-2, Marunouchi, 2-chome Chiyoda-ku
Tokyo 100(JP)

(72) Inventor: Yoshizawa, Yoshihito
450-3, Niiborishinden
Kumagaya-shi Saitama(JP)
Inventor: Yamauchi, Kiyotaka
153, Beppu 5-chome
Kumagaya-shi Saitama(JP)

(74) Representative: Strehl, Schübel-Hopf,
Groening, Schulz
Maximilianstrasse 54 Postfach 22 14 55
D-8000 München 22(DE)

(54) Magnetic core and method of producing same.

(57) A magnetic core made of an Fe-base soft magnetic alloy consisting essentially of Fe, Cu and M wherein M is at least one of the elements, Nb, W, Ta, Zr, Hf, Ti and Mo, at least 50% of the alloy structure being occupied by fine crystalline particles, and the change ratio X of the effective permeability with time of said magnetic core being o.3 or less, where X is defined by the following formula:

$X = 1 - \mu_b / \mu_a$

wherein μ_a is the effective permeability at 1 kHz, and μ_b is the effective permeability at 1 kHz after heating at 100 °C for 1000 hours in the air.

EP 0 299 498 A1

BACKGROUND OF THE INVENTION

The present invention relates to a magnetic core having good magnetic characteristics which are less changeable with time, and more particularly to a magnetic core for semiconductor circuit reactors, common mode chokes transformers, motors, etc.

Magnetic cores for the above applications are generally required to have small magnetostriction, high effective permeability and a high saturation magnetic flux density, and also it is required that these magnetic properties are less changeable with time, meaning that they have good durability.

In addition to the above characteristics, particularly when used as a saturable reactor for a magnetic amplification circuit, the magnetic cores are required to have a low core loss and good control magnetization characteristics (a low uncontrollable magnetic flux density).

A semiconductor circuit reactor is used to prevent electric current larger than a rated value from flowing through a semiconductor circuit due to current spike or electric linking generated by on and off of the semiconductor circuit, thereby avoiding the breakage of the semiconductor circuit, and also to prevent errors due to noises. Thus, such a reactor is particularly required to have high effective permeability and a high squareness ratio to suppress the above abnormal current.

For a common mode choke, a magnetic core should have a large operable effective magnetic flux range to prevent a monopolar noise, and it should have a small squareness ratio of a DC B-H curve.

For a transformer, a magnetic core should have a small squareness ratio of a DC B-H curve to prevent a monopolar noise as in a common mode choke, and it is required to have excellent high-frequency characteristics, particularly a small core loss at high frequency, because recent switching power supplies have been getting operated at higher frequency.

Recently, as such materials of having saturation magnetic flux density, Fe-base and Co-base amorphous alloys have been getting much attention. Co-base amorphous alloys have a small magnetostriction and high effective permeability. Their use for saturable reactors were proposed by Japanese Patent Laid-Open Nos. 57-210612 and 57-21512. On the other hand, Fe-base amorphous alloys have higher saturation magnetic flux density than Co-base amorphous alloys and also Fe-base amorphous alloys can have high squareness ratio when heat-treated in a non-oxidizing atmosphere as described in Japanese Patent Publication No. 58-1183.

Despite the fact that the Fe-base amorphous alloys have higher saturation magnetic flux density than the Co-base amorphous alloys, the former alloys are inferior to the latter alloys in a core loss and control magnetization characteristics, particularly when they are used for a saturable reactor in a magnetic amplification circuit of a switching power supply operated at a high frequency of 20 kHz or more. Because the Fe-base amorphous alloys have large total control magnetization force, large control magnetization current is required to control output voltage, leading to temperature increase of the magnetic core, and also increasing a load of the control circuit, decreasing its efficiency, and making other parts nearby less durable. In addition, when a semiconductor circuit reactor is formed from an Fe-base amorphous alloy, it shows extremely high magnetostriction and low effective permeability, so that spike current, etc. cannot effectively be prevented.

In the meantime, a transformer of a switching power supply is conventionally made of Mn-Zn ferrite, but it was proposed by Denkitsushin Gakkai Technical Report PE 84-3812 to use an Fe-base amorphous alloy for a transformer of a switching power supply operable at high frequency. However, as this Technical Report points out, when an Fe-base amorphous alloy is used, the core shows large magnetostriction, which leads to deterioration of magnetic properties by mechanical stress, and also the deterioration of high-frequency magnetic characteristics takes place when the core is cut or impregnated with a resin.

Accordingly, it has been desired to provide a material which has low magnetostriction and high effective permeability comparable to those of Co-base amorphous alloys and high saturation magnetic flux density comparable to that of the Fe-base amorphous alloys, such characteristics being substantially unchangeable with time.

Japanese Patent Laid-Open No. 62-101008 discloses a pseudo-crystalline material having fine crystalline particles of 0.1 μ m or less uniformly dispersed in an amorphous matrix phase in a volume larger than that of the matrix phase, which may be used as a magnetic core with magnetic characteristics little changeable with time in a magnetic circuit. This pseudo-crystalline material has improved heat resistance, but its magnetic properties are not so improved.

OBJECT AND SUMMARY OF THE INVENTION

Therefore, an object of the present invention is to provide a magnetic core having high saturation magnetic flux density and effective permeability and a low core loss. As a result of intense research, the inventors have found that such a magnetic core can be produced from an Fe-base soft magnetic alloy consisting essentially of Fe, Cu and M, wherein M is at least one element selected from the group consisting of Nb, W, Ta, Zr, Hf, Ti and Mo, at least 50% of the alloy structure being occupied by fine crystalline particles, the magnetic core having a change ratio of effective permeability with time (X) of 0.3 or less.

BRIEF DESCRIPTION OF THE DRAWINGS

Fig. 1 is a graph showing the effective permeability μ_{ek} of magnetic cores changing with time;

Fig. 2 is a graph showing the X-ray diffraction pattern of the Fe-base alloy ribbon manufactured by a single roll method in Example 1;

Fig. 3 (a) is a graph showing the X-ray diffraction pattern of the Fe-base alloy ribbon heat-treated in Example 1;

Fig. 3 (b) is a transmission electron photomicrograph of the Fe-base alloy ribbon heat-treated in Example 1;

Figs. 4 (a)-(h) are graphs showing various heat treatment patterns in which "a" denotes rapid heating and "b" denotes air cooling;

Fig. 5 is a perspective view showing a toroidal wound core of the Fe-base alloy ribbon in Example 1;

Fig. 6 is a schematic view showing a circuit for measuring the control magnetization properties of a magnetic core;

Fig. 7 is a graph showing the characteristics of a magnetic core as a saturable reactor;

Fig. 8 is a graph showing the relation between ΔB and a magnetic field H;

Fig. 9 is a graph showing the relation between a core loss and frequency;

Fig. 10 is a graph showing the relation between ΔB_b, ΔB and a magnetic field H;

Fig. 11 is a graph showing the relations between B_{10}, B_r/B_{10}, core loss and Hc and temperature;

Fig. 12 is a graph showing the relations between output voltage, η and temperature increase ΔT at a core case surface and current at a 12V load;

Figs. 13 (a)-(c) are graphs each showing a DC B-H curve;

Fig. 14 is a graph showing the relation between a specific core gain G_0 and X (atomic %);

Fig. 15 is a graph showing the relation between a specific core gain G_0 and α (atomic %);

Fig. 16 is a perspective view showing a semiconductor circuit reactor;

Fig. 17 is a schematic view showing a basic circuit of a switching power supply using the semiconductor circuit reactor of Fig.16;

Fig. 18 is a graph showing the wave forms of load current, in which A denotes a case where the semiconductor circuit reactor of the present invention is not used, and B denotes a case where the reactor is used;

Fig. 19 is a schematic view showing an example of a semiconductor circuit reactor including the reactor of the present invention;

Fig. 20 is a schematic view showing an example of a common mode choke;

Fig. 21 is a graph showing the relation between a noise level and frequency;

Fig. 22 (a) is a perspective view showing a toroidal wound core;

Fig. 22 (b) is a perspective view showing a magnetic core produced from the toroidal wound core of Fig. 22(a);

Fig. 23 (a) is a graph showing a DC B-H curve;

Fig. 23 (b) is a graph showing the relation between pulse permeability μ, and ΔB;

Fig. 24 is a graph showing the relation between the absolute value of complex permeability $|\mu|$ and frequency;

Fig. 25 (a) is a perspective view showing an E core;

Fig. 25 (b) is a perspective view showing an E-type magnetic core for a transformer;

Fig. 26 (a) is a schematic view showing a circuit for evaluating pulse attenuation characteristics;

Fig. 26 (b) is a graph showing the relation between output pulse peak voltage and input pulse peak voltage;

Fig. 27 (a) is a schematic view showing a circuit for measuring the dependency of attenuation on frequency;

Fig. 27 (b) is a graph showing the relation between attenuation and frequency;

Fig. 28 (a) is a perspective view showing a toroidal wound core;

Fig. 28 (b) is a perspective view showing a cut core; and

Fig. 29 is a graph showing the relation between a core loss and frequency.

DETAILED DESCRIPTION OF THE INVENTION

The magnetic core of the present invention having a change ratio of effective permeability with time (X) of 0.3 or less is generally produced from an Fe-base soft magnetic alloy consisting essentially of Fe, Cu and M, wherein M is at least one element selected from the group consisting of Nb, W, Ta, Zr, Hf, Ti and Mo, at least 50% of the alloy structure being occupied by fine crystalline particles.

Specifically, the Fe-base soft magnetic alloy used for the magnetic core according to the present invention may generally have the composition represented by the general formula:

$(Fe_{1-a}M_a)_{100-x-y-z-\alpha}Cu_xSi_yB_zM'_\alpha$

wherein M is Co and/or Ni, M' is at least one element selected from the group consisting of Nb, W, Ta, Zr, Hf, Ti and Mo, and a, x, y, z and α respectively satisfy $0 \leq a \leq 0.5$, $0.1 \leq x \leq 3$, $0 \leq y \leq 30$, $0 \leq z \leq 25$, $5 \leq y+z \leq 30$ and $0.1 \leq \alpha \leq 30$, at least 50% of the alloy structure being occupied by fine crystalline particles.

Another type of an Fe-base soft magnetic alloy suitable for the present invention has the composition represented by the general formula:

$(Fe_{1-a}M_a)_{100-x-y-z-\alpha-\beta-\gamma}Cu_xSi_yB_zM'_\alpha M''_\beta X_\gamma$

wherein M is Co and/or Ni, M' is at least one element selected from the group consisting of Nb, W, Ta, Zr, Hf, Ti and Mo, M'' is at least one element selected from the group consisting of V, Cr, Mn, At , elements in the platinum group, Sc, Y, rare earth elements, Au, Zn, Sn and Re, X is at least one element selected from the group consisting of C, Ge, P, Ga, Sb, In, Be and As, and a, x, y, z , α, β and γ respectively satisfy $0 \leq a \leq 0.5$, $0.1 \leq x \leq 3$, $0 \leq y \leq 30$, $0 \leq z \leq 25$, $5 \leq y+z \leq 30$, $0.1 \leq \alpha \leq 30$, $\beta \leq 10$ and $\gamma \leq 10$, at least 50% of the alloy structure being fine crystalline particles having an average particle size of 1000 Å or less.

In each of the above Fe-base soft magnetic alloys, Fe may be substituted by Co and/or Ni in the range of up to 0.3. When M (Co and/or Ni) exceeds 0.3, the magnetic core's control magnetization properties deteriorate. However, to have good magnetic properties such as low core loss and magnetostiction, the content of Co and/or Ni which is represented by "a" is preferably 0-0.1. Particularly to provide a low-magnetrostriction alloy, the range of "a" is preferably 0-0.05.

Cu is an indispensable element, and its content "x" is 0.1-3 atomic %. When it is less than 0.1 atomic %, substantially no effect on the reduction of core loss and on the increase in permeability can be obtained by the addition of Cu. On ther other hand, when it exceeds 3 atomic %, the resulting magnetic core's control magnetization properties become lower than those containing no Cu. The preferred content of Cu in the present invention is 0.5-2 atomic %, in which range the magnetic core can have control magnetization properties comparable to those of Co-base amorphous alloy magnetic cores.

The reasons why the core loss decreases and the permeability increases by the addition of Cu are not fully clear, but it may be presumed as follows:

Cu and Fe have a positive interaction parameter so that their sulubility is low. Accordingly, when the alloy is heated while it is amorphous, iron atoms or copper atoms tend to gather to form clusters, thereby producing compositional fluctuation. This produces a lot of domains likely to be crystallized to provide nuclei for generating fine crystalline particles. These crystalline particles are based on Fe, and since Cu is substantially not soluble in Fe, Cu is ejected from the fine crystalline particles, whereby the Cu content in the vicinity of the crystalline particles becomes high. This presumably suppresses the growth of crystalline particles.

Because of the formation of a large number of nuclei and the suppression of the growth of crystalline particles by the addition of Cu, the crystalline particles are made fine, and this phenomenon is accelerated by the inclusion of Nb, Ta, W, Mo, Zr, Hf, Ti, etc.

Without Nb, Ta, W, Mo, Zr, Hf, Ti, etc., the crystalline particles are not fully made fine and thus the soft magnetic properties of the resulting alloy are poor. Particularly Nb and Mo are effective, and particularly Nb acts to keep the crystalline particles fine, thereby providing excellent soft magnetic properties. And since a fine crystalline phase based on Fe is formed, the Fe-base soft magnetic alloy has smaller magnetostriction than Fe-base amorphous alloys, which means that the Fe-base soft magnetic alloy has smaller magnetic anisotropy due to internal stress-strain, resulting in improved soft magnetic properties.

Without the addition of Cu, the crystalline particles are unlikely to be made fine. Instead, a compound phase is likely to be formed and crystallized, thereby deteriorating the magnetic properties.

Si and B are elements particularly for making fine the alloy structure. The Fe-base soft magnetic alloy is desirably produced by once forming an amorphous alloy with the addition of Si and B, and then forming fine crystalline particles by heat treatment.

The content of Si ("y") and that of B ("z") are $0 \leq y \leq 30$ atomic %, $0 \leq z \leq 25$ atomic %, and $5 \leq y+z \leq 30$ atomic %, because the alloy would have an extremely reduced saturation magnetic flux density if otherwise.

In the present invention, the preferred range of y is 6-25 atomic %, and the preferred range of z is 2-25 atomic %, and the preferred range of y + z is 14-30 atomic %. When y exceeds 25 atomic %, the resulting alloy has a relatively large magnetostriction under the condition of providing good soft magnetic properties, and when y is less than 6 atomic %, sufficient soft magnetic properties are not necessarily obtained. The reasons for limiting the content of B ("z") is that when z is less than 2 atomic %, uniform crystalline particle structure cannot easily be obtained, somewhat deteriorating the soft magnetic properties, and when z exceeds 25 atomic %, the resulting alloy would have a relatively large magnetostriction under the heat treatment condition of providing good soft magnetic properties. With respect to the total amount of Si + B (y + z), when y + z is less than 14 atomic %, it is often difficult to make the alloy amorphous, providing relatively poor magnetic properties, and when y + z exceeds 30 atomic % an extreme decrease in a saturation magnetic flux density and the deterioration of soft magnetic properties and the increase in magnetostriction ensue. More preferably, the contents of Si and B are $10 \leq y \leq 25$, $3 \leq z \leq 18$ and $18 \leq y+z \leq 28$, and this range provides the alloy with excellent soft magnetic properties, particularly a saturation magnetostriction in the range of $-5 \times 10^{-6} - +5 \times 10^{-6}$. Particularly preferred ranges are $11 \leq y \leq 24$, $3 \leq z \leq 9$ and $18 \leq y+z \leq 27$, and this range provides the alloy with a saturation magnetrostriction in the range of $-1.5 \times 10^{-6} - +1.5 \times 10^{-6}$.

In the present invention, M′, when added together with Cu, acts to make the precipitated crystalline particles fine. M′ is at least one element selected from the group consisting of Nb, W, Ta, Zr, Hf, Ti and Mo. These elements have a function of elevating the crystallization temperature of the alloy. Synergistically with Cu having a function of forming clusters and thus lowering the crystallization temperature, Nb, etc. suppress the growth of the precipitated crystalline particles, thereby making them fine.

The content of M′ (α) is 0.1-30 atomic %. When it is less than 0.1 atomic %, sufficient effect of making crystalline particles fine cannot be obtained, and when it exceeds 30 atomic % an extreme decrease in saturation magnetic flux density ensues. The preferred content of M′ is 0.1-10 atomic %, and more preferably α is 2-8 atomic %, in which range particularly excellent soft magnetic properties are obtained. Incidentally, most preferable as M′ is Nb and/or Mo, and particularly Nb in terms of magnetic properties. The addition of M′ provides the Fe-base soft magnetic alloy with as high permeability as that of the Co-base, high-permeability materials.

M″, which is at least one element selected from the group consisting of V, Cr, Mn, Al, elements in the platinum group, Sc, Y, rare earth elements, Au, Zn, Sn and Re, may be added for the purposes of improving corrosion resistance or magnetic properties and of adjusting magnetostriction, but its content is at most 10 atomic %. When the content of M″ exceeds 10 atomic %, an extreme decrease in a saturation magnetic flux density ensues. A particularly preferred amount of M″ is 5 atomic % or less.

Among them, at least one element selected from the group consisting of Ru, Rh, Pd, Os, Ir, Pt, Au, Cr and V is capable of providing the alloy with particularly excellent corrosion resistance and wear resistance, thereby making it suitable for magnetic heads, etc.

The Fe-base soft magnetic alloy may contain 10 atomic % or less of at least one element X selected from the group consisting of C, Ge, P, Ga, Sb, In, Be, As. These elements are effective for making the alloy amorphous, and when added with Si and B, they help make the alloy amorphous and also are effective for adjusting the magnetostriction and Curie temperature of the alloy.

In sum, in the Fe-base soft magnetic alloy having the general formula:

$$(Fe_{1-a}M_a)_{100-x-y-z-\alpha}Cu_xSi_yB_zM'_\alpha$$

the general ranges of a, x, y, z and α are

$$0 \leq a \leq 0.5 \quad 0.1 \leq x \leq 3 \quad 0 \leq y \leq 30 \quad 0 \leq z \leq 25 \quad 5 \leq y+z \leq 30 \quad 0.1 \leq \alpha \leq 30,$$

and the preferred ranges thereof are

$$0 \leq a \leq 0.3 \quad 0.1 \leq x \leq 3 \quad 0 \leq y \leq 25 \quad 2 \leq z \leq 25 \quad 14 \leq y+z \leq 30 \quad 0.1 \leq \alpha \leq 10,$$

and the more preferable ranges are

$$0 \leq a \leq 0.1 \quad 0.5 \leq x \leq 2 \quad 10 \leq y \leq 25 \quad 3 \leq z \leq 18 \quad 18 \leq y+z \leq 28 \quad 2 \leq \alpha \leq 8,$$

and the most preferable ranges are

$$0 \leq a \leq 0.05 \quad 0.5 \leq x \leq 2 \quad 11 \leq y \leq 24 \quad 3 \leq z \leq 9 \quad 18 \leq y+z \leq 27 \quad 2 \leq \alpha \leq 8,$$

And in the Fe-base soft magnetic alloy having the general formula:

$(Fe_{1-a}M_a)_{100-x-y-z-\alpha-\beta-\gamma}Cu_xSi_yB_zM_\alpha M'_\beta X_\gamma$

the general ranges of a, x, y, z, α , β and γ are

$0 \leq a \leq 0.5$ $0 \leq x \leq 3$ $0.1 \leq y \leq 30$ $0 \leq z \leq 25$ $5 \leq y+z \leq 30$ $0.1 \leq \alpha \leq 30$ $\beta \leq 10$ $\gamma \leq 10$.

and the preferred ranges are

$0 \leq a \leq 0.3$ $0.1 \leq x \leq 3$ $6 \leq y \leq 25$ $2 \leq z \leq 25$ $14 \leq y+z \leq 30$ $0.1 \leq \alpha \leq 10$ $\beta \leq 5$ $\gamma \leq 5$.

and the more preferable ranges are

$0 \leq a \leq 0.1$ $0.5 \leq x \leq 2$ $10 \leq y \leq 25$ $3 \leq z \leq 18$ $18 \leq y+z \leq 28$ $2 \leq \alpha \leq 8$ $\beta \leq 5$ $\gamma \leq 5$,

and the most preferable ranges are

$0 \leq a \leq 0.05$ $0.5 \leq x \leq 2$ $11 \leq y \leq 24$ $3 \leq z \leq 9$ $18 \leq y+z \leq 27$ $2 \leq \alpha \leq 8$ $\beta \leq 5$ $\gamma \leq 5$.

The Fe-base soft magnetic alloy having the above composition has an alloy structure, at least 50% of which consists of fine crystalline particles. These crystalline particles are based on α -Fe having a bcc structure, in which Si and B, etc. are dissolved. These crystalline particles have an extremely small average particle size of 1000Å or less, and are uniformly distributed in the alloy structure. Incidentally, the average particle size of the crystalline particles is determined by measuring the maximum size of each particle and averaging them. When the average particle size exceeds 1000 Å , good soft magnetic properties are not obtained. It is preferably 500 Å or less, more preferably 200 Å or less and particularly 50-200 Å. The remaining portion of the alloy structure other than the fine crystalline particles may be mainly amorphous. Even with fine crystalline particles occupying substantially 100% of the alloy structure, the Fe-base soft magnetic alloy has sufficiently good magnetic properties.

Incidentally, with respect to inevitable impurities such as N, O, S, etc., it is to be noted that the inclusion thereof in such amounts as not to deteriorate the desired properties is not regarded as changing the alloy composition suitable for the magnetic cores of the present invention.

Next, the method of producing the Fe-base soft magnetic alloy will be explained in detail below.

First, an alloy melt of the above composition is rapidly quenched by known liquid quenching methods such as a single roll method, a double roll method, etc. to form amorphous alloy ribbons. Usually amorphous alloy ribbons produced by the single roll method, etc. have a thickness of 5-100 μ m or so, and those having a thickness of 25 μ m or less are particularly suitable as magnetic core materials for use at high frequency.

These amorphous alloys may contain crystal phases, but the alloy structure is preferably amorphous to make sure the formation of uniform fine crystalline particles by a subsequent heat treatment. Incidentally, the Fe-base soft magnetic alloy containing fine crystalline particles can be produced directly by the liquid quenching method without resorting to heat treatment, as long as proper conditions are selected.

The amorphous ribbons are wound, punched, etched or subjected to any other working to desired shapes before heat treatment, for the reasons that the ribbons have good workability in an amorphous state, but that once crystallized they lose such workability.

The heat treatment is carried out by heating the amorphous alloy ribbon worked to have the desired shape in vacuum or in an inert gas atmosphere such as hydrogen, nitrogen, argon, etc. The temperature and time of the heat treatment vary depending upon the composition of the amorphous alloy ribbon and the shape and size of a magnetic core made from the amorphous alloy ribbon, etc., but in general it is preferably 450-700°C for 5 minutes to 24 hours. When the heat treatment temperature is lower than 450 °C, crystallization is unlikely to take place with ease, requiring too much time for the heat treatment. On the other hand, when it exceeds 700°C , coarse crystalline particles tend to be formed, making it difficult to obtain fine crystalline particles. And with respect to the heat treatment time, when it is shorter than 5 minutes, it is difficult to heat the overall wound core at uniform temperature, providing uneven magnetic properties, and when it is longer than 24 hours, productivity becomes too low and also the crystalline particles grow excessively, resulting in the deterioration of magnetic properties. The preferred heat treatment conditions are, taking into consideration practicality and uniform temperature control, etc., 500-650°C for 5 minutes to 6 hours.

The heat treatment atmosphere is preferably an inert gas atmosphere, but it may be an oxidizing atmosphere such as the air. Cooling may be carried out properly in the air or in a furnace. And the heat treatment may be conducted by a plurality of steps.

The heat treatment can be carried out in a magnetic field to provide the alloy with magnetic anisotropy. When a magnetic field is applied in parallel to the magnetic path of the magnetic core of the present invention in the heat treatment step, the resulting heat-treated magnetic core has a good squareness ratio in a B-H curve thereof, so that it is particularly suitable for saturable reactors, magnetic switches, pulse compression cores, reactors for preventing spike voltage, etc. On the other hand, when the heat treatment

is conducted while applying a magnetic field in perpendicular to the magnetic path of a magnetic core, the B-H curve inclines, providing it with a small squareness ratio and a constant permeability. Thus, it has a wider operational range and thus is suitable for transformers, noise filters, choke coils, etc.

The magnetic field need not be applied always during the heat treatment, and it is necessary only when the alloy is at a temperature lower than the Curie temperature Tc thereof. In the present invention, the alloy has an elevated Curie temperature because of crystallization than the amorphous counterpart, and so the heat treatment in a magnetic field can be carried out at temperature higher than the Curie temperature of the corresponding amorphous alloy. In a case of the heat treatment in a magnetic field, it may be carried out by two or more steps. Also, a rotational magnetic field can be applied during the heat treatment.

The magnetic core of the present invention preferably has a saturation magnetic flux density B_s of 10kG or more and effective permeability μ_{e1kHz} of 5×10^3 or more.

In the present invention, a change ratio of effective permeability with time (X) is defined by the following formula:

$$X = 1 - \mu_b \mu_a$$

wherein μ_a is effective permeability at 1kHz of a sample before test and μ_b is effective permeability at 1kHz of a sample after a test of heating it at 100°C for 1000 hours in the air. The heating test can be conducted in a constant-temperature furnace.

This change ratio X should be 0.3 or less, and is preferably 0.1 or less and more preferably 0.05 or less.

As described above, to avoid the deterioration of magnetic characteristics of the magnetic core by internal stress generated when impregnated or coated with a resin, it is desirable that the magnetic core has saturation magnetostriction λs of $+5 \times 10^{-6} \sim -5 \times 10^{-6}$, and more particularly $+1.5 \times 10^{-6} \sim -1.5 \times 10^{-6}$.

By using the Fe-base soft magnetic alloy having the above composition and characteristics, a saturable reactor, a semiconductor circuit reactor, a common mode choke, a normal mode choke, a high-frequency transformer, a motor core, etc. can be provided.

In the case of a saturable reactor or a semiconductor reactor, the former should have a large controllable range and the latter should prevent spike current without reducing the voltage to be applied to the circuit. Therefore, the magnetic core for both reactors should have a squareness ratio B_r/B_{10} of a DC B-H curve which is desirably 70% or more and particularly 80% or more. Incidentally, B_r means a residual magnetic flux density and B_{10} means a magnetic flux density at 10 Oe which is almost equal to a saturation magnetic flux density. Such a high squareness ratio can be obtained by heat treatment while applying a magnetic field in parallel with the magnetic path of the magnetic core.

For a saturable reactor, it is desired that the magnetic core has an uncontrollable magnetic flux density ΔB_b of 3kG or less at 50kHz to prevent voltage from changing when load current increases.

When the magnetic core of the present invention is used for a reactor for a semiconductor circuit, it shows an excellent function of preventing spike voltage from flowing through the semiconductor circuit.

When it is used for a common mode choke or a high- frequency transformer, a large effective magnetic flux density range can be achieved to a mono-polar pulse voltage input. Accordingly, its DC B-H curve desirably has a squareness ratio B_r/B_{10} of 30% or less.

To reduce a core loss, it is desired that either or both of the ribbon surfaces are partially or totally coated with an insulating layer. This insulating layer can be formed by various method. For instance, it can be formed by attaching insulating powder such as SiO_2, MgO, Al_2O_3, etc. to the ribbon surface by immersion, spraying, electrophoresis, etc. A thin layer of SiO_2, etc. may be formed by sputtering or vapor deposition. Alternatively, a mixture of a solution of modified alkylsilicate in alcohol with an acid may be applied to the ribbon. Further, a forsterite ($MgSiO_4$) layer may be formed by heat treatment. Further, a sol obtained by partially hydrolyzing SiO_2-TiO_2 metal alkoxide may be mixed with various ceramic powder, and the resulting mixture may be applied to the ribbon. Further, a solution mainly containing a polytitanocarbosilane may be applied to the ribbon and then heated. Further, a phosphate solution may be applied and heated. In addition, the insulating layer may be formed by applying an oxidizing agent to the ribbon and heating it.

For the purpose of producing a saturable reactor, etc. from the wound core, the wound core may consist of the alloy ribbon and an insulating tape interposed between the adjacent ribbon layers. This wound core can be formed by laying the insulating tape on the ribbon and winding them. This insulating tape may be a polyimide tape, a ceramic fiber insulating tape, a polyester tape, an aramide tape, a glass fiber tape, etc.

When a highly heat-insulating tape is used, the wound core containing such tape may be subjected to heat treatment.

In the case of laminated core, an insulating thin film is inserted between the adjacent layers to achieve insulating between the alloy sheet layers. In this case, materials having no flexibility, such as ceramics, glass, mica, etc. may be used for the insulating thin film. When these materials are used, heat treatment can be conducted after lamination.

In the case of a wound core, an inner end and an outer end of the ribbon should be fixed to the wound core body to prevent loosening of the wound core. The fixing of the ribbon ends can be conducted by applying a laser beam or electric energy to a spot for fixing, or by using an adhesive or an adhesive tape.

Incidentally, the Fe-base soft magnetic alloy ribbon is desirably plated or coated to prevent corrosion. Further, the wound core may be contained in an insulating case, and such a material as grease can be used to fill a space between the wound core and the case to ensure the insulation and anti-corrosion of the wound core. Because the magnetic core of the present invention is made of an Fe-base alloy, its isolation from the air is particularly important.

The present invention will be explained in detail by the following Examples, without intention of restricting the scope of the present invention.

Example 1

A melt having a composition (by atomic %) of 1% Cu, 13.5% Si, 7.2% B, 2.5% Nb and balance substantially Fe was formed into a ribbon of 4.5 mm in width and 18 μm in thickness by a single roll method. The X-ray diffraction of this ribbon showed a halo pattern peculiar to an amorphous alloy in Fig. 2. A transmission electron photomicrograph of this ribbon also showed no crystal particles in the alloy structure. As is clear from the X-ray diffraction and the transmission electron photomicrograph, the resulting ribbon was almost completely amorphous.

Next, this amorphous ribbon was formed into a toroidal wound core of 10 mm in inner diameter and 13 mm in outer diameter as shown in Fig. 5, and then heat-treated in a nitrogen gas atmosphere at 550 °C for one hour.

This toroidal wound core was contained in a core case made of a phenol resin, and 10 turns of wires were wound around it on both primary and secondary sides. This magnetic core was placed in a constant-temperature furnace at 100 °C to measure the change of its effective permeability with time. The results are shown in Fig. 1, in which A_1 denotes the magnetic core of this Example. For comparison, an amorphous alloy having the composition (by atomic %) of 0.4% Fe, 5.9% Mn, 15% Si, 9% B and balance substantially Co and an Fe-base amorphous alloy having the same composition as A_1 (this Example) without heat treatment was formed into magnetic cores in the same manner as above, and their effective permeability was measured with the lapse of time. The results are also shown in Fig. 1, in which B_1 denotes the magnetic core made of the Co-base amorphous alloy and C_1 the magnetic core made of the Fe-base amorphous alloy ($Fe_{bal}Cu_1Nb_{2.5}Si_{13.5}B_{7.2}$) which was not heat-treated.

It is clear from Fig. 1 that effective permeability did not substantially change with time for the magnetic core of the present invention (change ratio of effective permeability with time $x = 0.02$), while x was as high as 0.73 for the magnetic core of the Co-base amorphous alloy (Comparative Example). And in the case of the Fe-base amorphous alloy having the same composition, x was as low as 0.03, but its effective permeability itself was too low to be used for magnetic cores. Thus, it has been verified that the magnetic core of the present invention has excellent durability due to a low change ratio of effective permeability with time.

The magnetic core of the present invention was decomposed to analyze the metal structure of its ribbon by X-ray diffraction and transmission electron microscopy. Fig. 3(a) shows the X-ray diffraction pattern of the Fe-base alloy of this Example, and Fig. 3(b) schematically shows the transmission electron photomicrograph of the same Fe-base alloy in which 1 denotes fine crystalline particles or grains and 2 a matrix phase. It is presumed that this matrix phase is amorphous, but when the heat treatment temperature is high, it may be converted to a fine crystal phase.

It has been confirmed from the X-ray diffraction pattern and the transmission electron photomicrograph that the Fe-base alloy of this Example contains extremely fine crystalline particles made of a bcc Fe solid solution having a particle size of 50-200 Å.

Example 2

This Example shows the measurement of control magnetization properties of a magnetic core.

Fig. 6 shows a circuit for measuring the control magnetization properties. which is equivalent to that for evaluating a saturable reactor. Fig. 7 is a schematic view showing the characteristics of a saturable reactor when DC control current Ic flows through the control circuit. In Fig. 6, sample S is a saturable reactor constituted by a magnetic core and 3 windings N_L, N_c and N_v.

N_L, which corresponds to an output winding of the saturable reactor used in the magnetic amplifier, is connected to an AC power source Eg having a frequency f (period: Tp) via resistor R_L and rectifier D. The value of Eg is set such that the magnetic core becomes saturated at a phase angle within 90° of applied sinusoidal voltage in a half-period Tg of a gate.

N_c is a control winding, and it is connected to DC power source Ec via inductor L_c having sufficiently large inductance as compared to the inductance of the magnetic core to give DC magnetization to the magnetic core.

N_v is a winding for measuring reset magnetic flux $\Delta \phi$ cm corresponding to control input, and it is connected to an AC voltmeter of a mean value rectification type.

Fig. 7 schematically shows a control magnetization curve measured by this circuit.

By defining a reciprocal number of a total control magnetization force Hr as β_0,

$\beta_0 = 1/Hr$

For a saturable reactor, the larger β_0 (the smaller Hr), the smaller control current, resulting in better characteristics.

On the other hand, a parameter α_0 showing a squareness ratio of a magnetization curve of a magnetic core is defined as follows:

$\alpha_0 = 1 - \Delta B_b/\Delta B_m$

For a saturable reactor, the larger α_0, the smaller an uncontrollable magnetic flux density ΔB_b, resulting in better characteristics.

The product of α_0 and β_0 is expressed by a specific core gain G_0:

$G_0 = \alpha_0 \cdot \beta_0$

The larger G_0, the more suitable the magnetic core is for a saturable reactor on the whole.

The maximum value B_m of a magnetic flux density corresponds to the maximum value of a gate magnetic field:

$H_{Lm} = \{N_L \cdot i_{L(max)}\}/l_e$ (1)

where l_e is an average magnetic path length of a sample.

A magnetic flux density B_c is determined by a control magnetic field:

$H = (N_c \cdot I_c)/l_e$ (2)

Difference between the maximum value B_m and the magnetic flux density B_c is expressed as ΔB_{cm}, and the reading E_v of a magnetic flux voltmeter V in the N_v circuit is as follows:

$E_v \propto f \cdot N_v \cdot A \cdot \Delta B_{cm}$ (3)

where f is a frequency and A is an effective cross-sectional area of the magnetic core.

In an actual saturable reactor, it is necessary to know H_{Lm} - ΔB_b characteristics in a positive region of a magnetic field H and H_{Lm} - ΔB_b characteristics in a negative region of a magnetic field H.

$\Delta B_b = B_m - B_r$ (4)

and

$E_{vd} \propto f \cdot N_v \cdot A \cdot \Delta B_b$ (5)

On the other hand,

$\Delta B = \Delta B_{cm} - \Delta B_b$ (6)

It is desirable for a saturable reactor that in Fig. 8, the curve is low in the first quadrant and it is near the axis and steeply inclined in the second quadrant.

Example 3

A melt having a composition (by atomic %) of 1% Cu, 13.5% Si, 9% B, 3% Nb and balance substantially Fe was formed into a ribbon of 4.5 mm in width and 18 μ m in thickness by a single roll method. This ribbon was almost completely amorphous. This ribbon was formed into a toroidal wound core of 10 mm in inner diameter and 13 mm in outer diameter. This alloy had a crystallization temperature of 508° C when measured at a heating rate of 10 °C /min and a Curie temperature of about 310° C.

Next, various patterns of heat treatment as shown in Figs. 4 (a)-(h) were conducted on each wound core

in a magnetic field. When a magnetic field was applied, it was in parallel with the magnetic path of the magnetic core at a level of 10 Oe. It was confirmed that the alloy after heat treatment had fine crystalline particles of 100 ~ 200 Å composed substantially of a bcc Fe solid solution and occupying a majority of the alloy structure.

Each wound core was contained in a phenol resin core case, and 10 turns of wires were wound around each magnetic core on both primary and secondary sides to provide a saturable reactor as in Example 1. The characteristics of each magnetic core were measured. The results are shown in Table 1.

Table 1

Heat Treatment Condition	B_{10} (kG)	B_r/B_{10} (%)	H_c (Oe)	$W_{2/100k}$ (mW/cc)
(a)	12.4	70	0.008	340
(b)	12.4	90	0.005	790
(c)	12.4	82	0.007	610
(d)	12.4	87	0.005	820
(e)	12.4	83	0.005	680
(f)	12.4	83	0.006	680
(g)	12.4	91	0.007	810
(h)	12.4	88	0.008	780

As is shown in Table 1, each pattern of heat treatment shown in Fig. 4 can provide the resulting magnetic core with high squareness ratio, and their core losses $W_{2/100k}$ at 2kG and 100 kHz were as small as those of Co-base amorphous alloy magnetic cores ($W_{2/100k}$ = 200 ~ 900). And their magnetic flux densities at 10 Oe (≒ B_s) were 12.4 kG, considerably higher than those of Co-base amorphous alloys, 80% Ni permalloy, etc.

Incidentally, the alloy heat-treated by the pattern (b) in Fig. 4 had a Curie temperature Tc of 570 °C and saturation magnetostriction λ s of 3.8×10^{-6}.

Example 4

A melt having a composition (by atomic %) of 1% Cu, 13.5% Si, 9% B, 5% Nb and balance substantially Fe was formed into a ribbon of 5 mm in width and 18 μ m in thickness by a single roll method. This alloy had a crystallization temperature of 533 °C when measured at a heating rate of 10 °C/min. And its Curie temperature was 260 °C.

Next, this ribbon was coated with MgO powder by electrophoresis, and formed into a wound core of 19 mm in outer diameter and 15 mm in inner diameter. This wound core was heated at 610 °C for 1 hour in an N_2 gas atmosphere, and cooled to 250 °C at a cooling rate of 5 °C/min in a magnetic field of 5 Oe in parallel with the magnetic path of the magnetic core. After keeping it at 250 °C for 4 hours, it was cooled to room temperature at a cooling rate of about 60 °C/min.

Another wound core of the same composition and the same structure was heated at 610 °C for 1 hour, and then cooled to room temperature at a cooling rate of 100 °C/min in a magnetic field of 5 Oe in parallel with the magnetic path of the magnetic core.

Each of these cores was contained in a phenol resin core case, and 10 turns of wires were wound around each magnetic core on both primary and secondary sides to provide a saturable reactor. The characteristics of each saturable reactor were tested. The results are shown in Table 2.

Table 2

	Heat Treatment Condition	B_s (kG)	B_r/B_{10} (%)	H_c (Oe)	$W_{2/100k}$ (mW/cc)
(a)	610℃ × 1h ↓ 250℃ × 4h(Hφ =50e)	11.3	89	0.007	680
(b)	610℃ × 1h→ R.T. (Hφ =50e)	11.3	87	0.006	380

As is clear from Table 2, these magnetic cores have high squareness ratio suitable for a saturable reactor. Incidentally, the alloy heat-treated by the pattern (b) had a main phase having a Curie temperature of 550° C and saturation magnetostriction λ s of 1 × 10^{-6}.

Further, it was observed that extremely fine crystalline particles existed predominantly in the alloy structure as in Example 1.

Example 5

Saturable reactors were produced by using an $Fe_{73.5}Cu_1Nb_3Si_{13.5}B_9$ alloy A_2, an $Fe_{71.5}Cu_1Nb_5Si_{13.5}B_3$ alloy A_3, an $Fe_{71.5}Cu_1Nb_5Si_{13.5}B_9$ alloy A_4, a high-squareness ratio Fe-base amorphous alloy C_2 - ($Fe_{69.3}Ni_{7.7}Si_{13}B_{10}$) and two high-squareness ratio Co-base amorphous alloys B_2, B_3 ($Co_{69.7}Fe_{0.4}Mn_{5.9}Si_{15}B_9$, $Co_{67}Fe_4Mo_{1.5}Si_{18.5}B_{11}$), respectively. The alloy A_2 was heat-treated by heating it at 550° C for 1 hour, cooling down to 280 °C and keeping it at that temperature for 1 hour while applying a magnetic field of 2 Oe in the direction of the magnetic path, the alloy A_3 was heat-treated by heating it at 610° C for 1 hour, cooling it down to 250° C and then keeping it at that temperature for 2 hours while applying a magnetic field of 15 Oe in the direction of the magnetic path, and the alloy A_4 was heat-treated by heating it at 610 °C for 1 hour and then air-cooling it while applying a magnetic field of 2 Oe in the direction of the magnetic path. Incidentally, B_r/B_{10} of each alloy was as follows:

	B_r/B_{10}(%)
ALLOY A_2	93
ALLOY A_3	89
ALLOY A_4	87
ALLOY C_2	90
ALLOY B_2	95
ALLOY B_3	85

Core loss was measured at 2 kG for each magnetic core of alloy A_2-B_3. The results are shown in Fig. 9. As a result, it was found that the magnetic cores (A_2, A_3, A_4) used in the saturable reactor of the present invention showed a core loss comparable to or lower than those of the conventional high-squareness ratio Co-base amorphous alloys B_2, B_3. Thus, they are suitable for a saturable reactor. Further, it showed a core loss which was half or less of that of the conventional high-squareness ratio Fe-base amorphous alloy C_2.

Example 6

The alloys A_2, A_3, A_4, B_2 and B_3 shown in Fig. 9 were used to provide saturable reactors, and their control magnetization characteristics were evaluated by the circuit shown in Fig. 6. In this case, the primary winding (N_v) and the secondary winding (N_L) were respectively 17 turns and the control winding (N_c) was 5 turns. The results are shown in Fig. 10. As is clear from Fig. 10, the saturable reactor of the present

invention had a control magnetization force comparable to that of high-squareness ratio Co-base amorphous alloy for the sameΔ B, but the former had a total controllable magnetic density ΔB_m 1.5 ~ 2 times as large as that of the Co-base amorphous alloy saturable reactor. Accordingly, the saturable reactor of the present invention can be miniaturized under the conditions that temperature increase of the core does not pose serious problems.

Example 7

A saturable reactor produced from a finely crystallized alloy consisting essentially of 1% Cu. 13.5% Si. 9% B, 3% Nb and substantially balance Fe (by atomic %), and the temperature characteristics of its magnetic properties were measured. The results are shown in Fig. 11.

Substantially no change was observed with respect to a squareness ratio, Br/B_{10}, a core loss, and a coercive force Hc in the range of room temperature to 150°C. With respect to B_{10}, it decreased by about 1 kG by temperature elevation from room temperature to 150°C , posing no practical problem. Thus, it has been verified that the saturable reactor produced from the above finely crystallized alloy had excellent durability.

Example 8

Alloy melts having compositions shown in Table 3 were formed into amorphous ribbons each having a width of 5 mm and a thickness of 18 μ m by a single roll method. Each ribbon was formed into a wound core of 19mm in outer diameter and 15 mm in inner diameter. Each wound core was heat-treated to form extremely fine crystalline particles in the alloy structure. The heat treatment conditions were according to the heat treatment pattern (b) in Fig. 4.

Each wound core was contained in a phenol resin core case and 10 turns of wires were wound around each wound core on both primary and secondary sides to provide a saturable reactor as in Example 1. For each magnetic core, a DC B-H curve, an AC B-H curve, a core loss $W_{2/100k}$ at 100 kHz and 2 kG, and control magnetization curve at 50 kHz were measured. Incidentally, the control magnetization curve was measured for a saturable reactor of the same structure as in Example 6 by a method shown in Example 2.

A magnetic flux density B_{10} at a magnetic field intensity of 10 Oe, a squareness ratio B_r/B_{10} of the DC B-H curve, Hc (DC), B_r/B_1 (AC) of the AC B-H curve at 20 kHz, Hc(AC), $W_{2/100k}$, a total control magnetization force Hr, and uncontrollable magnetic flux densityΔ Bb are shown in Table 3.

Table 3

No.*	Composition (at%)	$B_{1.0}$ (kG)	$Br/B_{1.0}$ (%)	Hc(DC) (Oe)	Br/B_1(AC) (%)	Ho(AC) (Oe)	$W_{2/1000}$ (mW/cc)	Hr (Oe)	ΔBb (kG)
1	$Fe_{73}Cu_{1.5}Si_{15.5}B_9Nb_2$	12.6	88	0.005	98	0.29	760	0.144	0.7
2	$Fe_{73}Cu_{0.5}Si_{15.5}B_9Mo_2$	12.4	80	0.012	94	0.28	780	0.148	1.4
3	$Fe_{73.5}Cu_1Si_{15.5}B_9Ta_2$	11.4	86	0.008	96	0.27	750	0.142	0.8
4	$Fe_{73}Cu_1Si_8B_9Nb_9$	14.6	80	0.020	94	0.32	880	0.167	1.3
5	$Fe_{73}Cu_2Si_{15.5}B_{9.5}Hf_2$	11.6	86	0.011	95	0.28	780	0.148	0.9
6	$Fe_{73}Cu_1Si_{14}B_9Zr_3$	11.7	85	0.012	96	0.28	770	0.146	0.9
7	$Fe_{71.5}Cu_1Si_{15.5}B_9Ti_3$	11.3	83	0.014	95	0.28	780	0.147	1.0
8	$Fe_{71}Cu_1Si_{15.5}B_9Nb_3V_{0.5}$	10.4	91	0.009	97	0.18	480	0.088	0.6
9	$Fe_{71}Cu_1Si_{17.5}B_9Nb_3Cr_{0.5}$	10.1	90	0.010	97	0.16	430	0.089	0.6
10	$Fe_{71}Cu_1Si_{13.5}B_{13}Nb_3Mn_{0.5}$	11.4	92	0.011	98	0.15	390	0.080	0.7
11	$Fe_{73.5}Cu_1Si_{15.5}B_6Nb_3C_3$	13.0	82	0.021	94	0.32	870	0.160	1.1
12	$Fe_{73}Cu_1Si_{10.5}B_{13}Nb_3Ge_{0.5}$	11.7	88	0.012	97	0.15	410	0.078	0.7
13	$Fe_{73.5}Cu_1Si_{15.5}B_9Nb_3Al_3$	11.5	87	0.014	97	0.28	780	0.146	0.8
14	$(Fe_{0.97}Ni_{0.03})_{73.5}Cu_1Si_{15.5}B_9Nb_2Ga_1$	12.3	87	0.011	97	0.29	790	0.150	0.8
15	$Fe_{63.5}Cu_1Si_{15.5}B_9Nb_7P_{3.5}$	9.6	86	0.017	97	0.31	850	0.161	0.9
16	$Fe_{73.5}Cu_1Si_{15.5}B_7Nb_3Ru_1$	13.2	90	0.010	98	0.29	800	0.152	0.6
17	$Fe_{73}Cu_1Si_{15.5}B_{11}Nb_3Y_{0.5}$	12.3	87	0.015	97	0.30	830	0.584	0.8
18	$Fe_{83.7}Cu_{7.7}Si_{15.5}B_9$ Amorphous	14.2	90	0.025	98	0.78	3000	0.67	0.8
19	$Co_{71}Fe_4Mo_{1.5}Si_{15.5}B_{11}$ Amorphous	5.5	85	0.003	96	0.16	400	0.085	0.6
20	$Co_{63.5}Fe_{6.5}Mn_{5.5}Si_{15}B_9$ Amorphous	7.8	95	0.004	99	0.34	900	0.181	0.4
21	50wt% Ni-Fe Permalloy	15.1	97	0.010	99	0.86	3800	0.85	0.3
22	80wt% Ni-Fe Permalloy	7.5	80	0.001	94	0.39	980	0.24	1.5

Note*: Sample Nos. 18-22 are Comparative Examples.

The saturable reactors of the present invention had higher B_{1c} than those of the Co-base amorphous alloys and 80 wt% Ni Permalloy, and the former had high squareness ratio. In addition, the saturable reactors of the present invention had excellent characteristics comparable to those of the Co-base amorphous alloys in Hc, a core loss, Hr and ΔB_b. Further, the saturable reactors of the present invention showed a low core loss compared to those produced from the 50 wt% Ni Permalloy and the Fe-base amorphous alloy, which means that the saturable reactor of the present invention has excellent control magnetization characterstics.

Because of these characteristics, the saturable reactor of the present invention can be operated by small control current, increasing the effenciency of a circuit. In addition, since ΔB_b is small, it enjoys a wide control range.

Example 9

Alloy melts having compositions shown in Table 4 were used to produce wound cores having extremely fine crystalline particles as in Example 8, and each wound core was formed into a saturable reactor. For each saturable reactor, a magnetic flux density B_{10} at 10 Oe, a core loss $W_{2\cdot100k}$ at 100 kHz and 2 kG, an uncontrollable magnetic flux density ΔB_b and saturation magnetostriction λs were measured. The results are shown in Table 4.

Table 4

No.*	Composition (at%)	B_{10} (kG)	Br/B_{10} (%)	Hc (Oe)	$W_{8/1000}$ (mW/cc)	Δ Bb (kG)	λ_s ($\times 10^{-6}$)
1	$(Fe_{0.993}Ni_{0.041})_{79.5}Cu_1Si_{13.5}B_8Nb_3$	12.3	90	0.008	890	0.6	+4.6
2	$Fe_{79.5}Cu_1Si_{13.5}B_8Nb_3$	10.8	88	0.012	820	0.7	~0
3	$(Fe_{0.993}Co_{0.04})_{79.5}Cu_1Si_{13.5}B_9Nb_2$	12.6	91	0.007	830	0.6	+4.0
4	$Fe_{79.5}Cu_1Si_{11.5}B_8Ta_3$	10.5	85	0.009	780	0.8	-0.3
5	$Fe_{71}Cu_{1.5}Si_{18.5}B_9Mo_5$	11.2	83	0.008	380	1.0	+1.9
6	$Fe_{71}Cu_1Si_{13}B_{10}W_5$	10.0	82	0.015	580	1.2	+2.5
7	$Fe_{76.5}Cu_1Si_{13.5}B_6Nb_5$	11.6	83	0.006	450	1.0	+1.5
8	$Fe_{71.5}Cu_1Si_{14.5}B_8Nb_5$	10.2	85	0.007	430	0.8	+2.0
9	$Fe_{68.75}Ni_{7.75}Si_{10.5}B_8$ Amorphous	14.2	90	0.025	3000	0.6	+29

Note*: Sample No. 9 is Comparative Example.

EP 0 299 498 A1

It is clear from Table 4 that the saturable reactor of the present invention has a high squareness ratio. low Hc, a low core loss, a low uncontrollable magnetic flux density ΔB_b than those of the Fe-base amorphous alloy. Further, since it has low λ s, the deterioration of magnetic characteristics by coating, etc. can be avoided.

Example 10

An amorphous alloy ribbon having a composition (by atomic %) of 1% Cu, 13.5% Si, 9% B, 3% Nb and balance substantially Fe, and an amorphous alloy ribbon having a composition (by atomic %) of 13.5% Si, 9% B, 3% Nb and balance substantially Fe were produced. The former amorphous alloy containing both Cu and Nb had a crystallization temperature of 508 °C when measured at a heating rate of 10 °C min, while the latter amorphous alloy (containing no Cu) had a crystallization temperature of 583 °C when measured under the same condition.

Each amorphous alloy ribbon was formed into a wound core of 19 mm in outer diameter and 15 mm in inner diameter. The wound core containing Cu-Nb according to the present invention was heated at 550 °C for 1 hour while applying a magnetic field of 10 Oe in the direction of its magnetic path and then cooled down to room temperature at a cooling rate of 20 °C min in order that extremely fine crystalline particles occupy a majority of the alloy structure. On the other hand, the magnetic alloy of the comparative example was heated at 500 °C for 1 hour and then cooled down to 280 °C at a cooling rate of 5 °C min while applying a magnetic field of 10 Oe in the direction of its magnetic path, and after keeping it at 280 °C for 4 hours, it was cooled down to room temperature at a cooling rate of 20 °C min. The wound core of the comparative example had an amorphous structure. Each of these wound cores was contained in a phenol resin core case, and formed into a saturable reactor by winding a primary wire and a second wire by 20 turns and a control wire by 5 turns.

Each saturable reactor was mounted in a magnetic control-type switching power supply having a driving frequency of 100 kHz. This switching power supply had two outputs; an output of 12 V (magnetic amplification control), and an output of 5 V (PWM control). By this switching power supply, the output characteristics of the saturable reactor were measured. Incidentally, input voltage was AC 100V, and while keeping load current of the 5 V output at constant, load current at the 12 V output was changed. In this case, 12 V output terminal voltage, power supply effeciency η and core case surface temperature increase Δ T were measured and compared between the two saturable reactors. The results are shown in Fig. 12, in which A_5 denotes the saturable reactor of the present invention and C_3 denotes the saturable reactor of the Fe-base amorphous alloy. It has been made clear that the saturable reactor of the present invention had smaller temperature increase and higher power supply efficiency η than those of comparative example (Fe-base amorphous alloy), with substantially no change in output voltage.

Example 11

A melt having a composition (by atomic %) of 0.8% Cu, 13.6% Si, 9% B, 3% Nb and balance Fe, and a melt having a composition (by atomic %) of 1% Cu, 13.5% Si, 9% B, 5% Nb, and balance Fe were formed into amorphous ribbons by a single roll method. Each of the amorphous ribbons was heat-treated in an N_2 gas atmosphere in a magnetic field of 10 Oe in the direction of the magnetic path thereof. The heat treatment conditions were heating at 550 °C for 1 hour, cooling to 280 °C , and keeping at 280 °C for 1 hour for the former alloy, and heating at 610 °C for 1 hour, cooling to 250 °C , and keeping at 250 °C for 4 hours for the latter alloy. The magnetic field was applied during the period of heat treatment. By this heat treatment, extremely fine crystalline particles were formed in the alloy structure.

Each wound core was contained in the Bakelite core case and 10 turns of wire were wound around each magnetic core on both primary and secondary sides to provide a saturable reactor. The characteristics of each saturable reactor were tested.

Fig. 13 shows a DC B-H curve for each saturable reactor, in which (a) is for the $Fe_{73.6}Cu_{0.8}Nb_3Si_{13.6}B_9$ alloy having B_{10} = 12.4kG, B_r/B_{10} = 93% and Hc = 0.004 Oe, and (b) is for the $Fe_{71.5}Cu_1Nb_5Si_{13.5}B_9$ alloy having B_{10} = 11.3kG, B_r/B_{10} = 90% and Hc = 0.007 Oe. For comparison, an amorphous alloy consisting essentially of 15% Si, 9% B, 5.9% Mn and balance substantially Co (by atomic %) was produced and formed into a saturable reactor. It had B_{10} = 7.8kG, B_r/B_{10} = 92% and Hc = 0.004 Oe. Fig. 13 (c) shows its

DC B-H curve. It is clear from Fig. 13 that the saturable reactors of the present invention (a) and (b) show higher B_{10} than that of the Co-base amorphous alloy (c) and they are almost equivalent in a coercive force Hc and a squareness ratio B_r/B_{10}. Further, the maximum permeability μ_{max} was 1450k for the $Fe_{73.5}Cu_{0.8}Si_{13.5}B_9Nb_3$ alloy and 1000k for the $Fe_{71.5}Cu_1Si_{13.5}B_9Nb_5$ alloy.

Example 12

An alloy melt of $Fe_{72.5-x}Cu_xSi_{13.5}B_9Nb_5$ (Alloy A_6) and an alloy melt of $Fe_{77.5-x}Cu_xSi_{13.5}B_9$ (Alloy A_7, comparative example) were formed into amorphous ribbons by a single roll method. Next, each ribbon was formed into a wound core of 19 mm in outer diameter and 15 mm in inner diameter, and the resulting wound core was heat-treated under the same conditions as in the heat treatment pattern in Fig. 4 while applying a magnetic field of 20 Oe in the direction of its magnetic path in an N_2 gas atmosphere. The heat-treated wound core was then contained in a phenol resin core case and 10 turns of wires were wound on primary and secondary sides to provide a saturable reactor. The saturable reactor was measured with respect to control magnetization characteristic in the circuit shown in Example 2.

Fig. 14 shows specific core gains G_0 measured at 50 kHz. For Alloy A_6 when x exceeds 0.1. G_0 increases extremely, but when x exceeds 3 G_0 undesirably decreases.

When Nd is not added (Alloy A_7), G_0 is not improved by the addition of Cu. This means that the addition of both Cu and Nd is extremely effective for improving the control magnetization characteristics of a saturable reactor.

Example 13

An alloy melt of $Fe_{78.5-\alpha}Cu_1Si_{15.5}B_7Nb_\alpha$ (Alloy A_8) and an alloy melt of $Fe_{77.5-\alpha}Si_{15.5}B_7Nb_\alpha$ (Alloy C_4) were formed into an amorphous ribbons by a single roll method. Next, each ribbon was formed into a wound core of 19 mm in outer diameter and 15 mm in inner diameter. Each wound core was heat-treated under the conditions as in the heat treatment pattern (b) in Fig. 4 while applying magnetic field of 20 Oe in the direction of the magnetic path in an N_2 gas atmosphere, and a saturable reactor was produced as in Example 12. Its specific core gain G_0 was measured at 50 kMz. The results are shown in Fig. 15. It has been verified from Fig. 15 that the saturable reactor of the present invention had extremely larger G_0 than comparative example, meaning that the addition of both Cu and Nd is remarkably effective for improving the control magnetization characteristics.

Example 14

A melt consisting of 1% Cu, 13.5% Si, 9% B, 3% Nb and balance substantially Fe by atomic % was formed into a ribbon of 3 mm in width and 18 μ m in thickness by a single roll method. This ribbon was subjected to a heat treatment shown by Fig. 4 (b) in Example 3. Next, this ribbon was formed into a wound core and then introduced into a phenol resin case. 20 turns of wires of 0.4 mm in diameter were wound around it to provide a reactor for semiconductor circuit shown in Fig. 16. This reactor was measured with respect to inductance at 1kHz. A ratio of the maximum inductance to the initial inductance was 3.03, and a ratio of the maximum inductance to a residual inductance was 300. Incidentally, the residual inductance is an inductance measured when DC current is applied.

Since the maximum inductance-residual inductance ratio is large, the reactor is excellent in improving the recovery characteristics of a diode.

Fig. 17 shows a basic circuit of a switching power supply using the above reactor. In Fig. 17, 10 denotes a main transformer, 11, 12, 13 each diode, 14 a smoothing choke, 15 the reactor of the present invention, and 16 a load. Input and output were both DC voltage. Fig. 18 shows the wave forms of load current. A denotes a case where no reactor was used, and B denotes a case where the reactor was inserted into a half-wave rectifier circuit operated at a pulse width of 10μ sec and input voltage of 100V DC. By using the reactor of the present invention, current spike was remarkably decreased.

Example 15

A melt having a composition (by atomic %) of 1% Cu. 13.5% Si, 7% B. 2.5% Nb and substantially balance Fe was formed into an amorphous ribbon of 3 mm in width and 18 μ m in thickness by a single roll method. The ribbon was coated with MgO powder on the side of contact with the single roll. to form an insulating layer. It was then wound to provide a toroidal wound core of 4 mm in outer diameter and 2 mm in inner diameter. This wound core was heat-treated at 550 °C for 1 hour. and its outer surface was coated with an epoxy resin and connected to diode terminals to provide a semiconductor circuit reactor combined with a diode as shown in Fig. 19. in which 20 denotes a diode and 21. 22 denote the reactors of the present invention.

Next, this reactor was used in a smoothing circuit on the output side of a switching power supply to measure diode voltage and output noise.

When the reactor of the present invention was not used, the diode voltage was 61.0 V and the output noise was 123 mVp-p. but when it was used the diode voltage was 33.5 V and the output noise was 47.3 mVp-p. Thus it was confirmed that the reactor of the present invention has excellent smoothing and noise reduction effects.

Example 16

Reactors were produced from alloy ribbons having compositions shown in Table 5 in the same manner as in Example 14, and their initial inductance L_0 and maximum inductance L_m were measured. After heat treatment at 120 °C for 1000 hours, their initial inductance $L_0'^{000}$ and maximum inductance $L_m'^{000}$ were also measured to determine ratios of $L_0'^{000}$ L_0 and $L_m'^{000}/L_m$. The results are shown in Table 5.

Table 5

No.*	Composition (at%)	L_o^{1000}/L_o	L_a^{1000}/L_a
1	$Fe_{bal.}Cu_1Si_{13.5}B_8Nb_3$	0.95	0.97
2	$Fe_{bal.}Cu_1Si_{13.5}B_7Mo_3$	0.97	0.97
3	$Fe_{bal.}Cu_1Si_{13.5}B_6Ta_3$	0.96	0.98
4	$Fe_{bal.}Cu_1Si_{13.5}B_5W_3$	0.97	0.97
5	$Fe_{bal.}Cu_1Si_{13.5}B_7Nb_2Ti_1$	0.96	0.97
6	$Fe_{bal.}Cu_1Si_{13.5}B_9Nb_2Zr_1$	0.95	0.95
7	$Fe_{bal.}Cu_1Si_{13.5}B_8Nb_2Hf_1$	0.96	0.97
8	$Fe_{bal.}Cu_1Si_{13.5}B_9Nb_2Cr_1$	0.96	0.95
9	$Fe_{bal.}Cu_1Si_{13.5}B_9Nb_{1.5}V_1$	0.95	0.95
10	$Fe_{bal.}Cu_1Si_{13}B_8Nb_3Al_3$	0.96	0.97
11	$Fe_{bal.}Cu_2Si_{17}B_5Nb_3$	0.99	0.98
12	$(Fe_{0.9}Co_{0.1})_{bal.}Cu_3Si_{13.5}B_9Nb_3$	0.98	0.97
13	$(Fe_{0.95}Co_{0.15})_{bal.}Cu_2Si_{13.5}B_9Nb_4$	0.97	0.96
14	$(Fe_{0.95}Ni_{0.05})_{bal.}Cu_2Si_{14}B_8Nb_3$	0.96	0.94
15	$(Fe_{0.9}Ni_{0.1})_{bal.}Cu_2Si_{14}B_7Nb_4$	0.97	0.95
16	$Fe_{bal.}Cu_{0.7}Si_{13}B_8Nb_3Mn_1$	0.95	0.95
17	$Fe_{bal.}Cu_1Si_{13}B_9Nb_3Ru_3$	0.99	0.99
18	$Fe_{bal.}Cu_1Si_7B_9Nb_3Zn_1$	0.96	0.95
19	$Fe_{bal.}Cu_1Si_6B_{10}Ta_2Sn_1$	0.96	0.94
20	$Fe_{bal.}Cu_1Si_{13}B_4Mo_3Re_1$	0.95	0.95
21	$Fe_{bal.}Cu_1Si_{12}B_8Nb_4C_1$	0.96	0.96
22	$Fe_{bal.}Cu_1Si_{13}B_{11}Nb_3Ge_3$	0.98	0.95
23	$Fe_{bal.}Cu_1Si_{13}B_8Nb_3Ga_3$	0.97	0.98
24	$Fe_{bal.}Cu_{1.5}Si_{17}B_6Nb_6$	0.96	0.96
25	$Fe_{bal.}Cu_1Si_{16}B_7Nb_2$	0.98	0.95
26	$Co_{bal.}Fe_4Mo_{1.5}Si_{16}B_{10}$ Amorphous	0.18	0.42
27	$Co_{bal.}Fe_{3.5}Mn_3Cr_4Si_{13}B_8$ Amorphous	0.17	0.40

Note *: Sample Nos. 26 and 27 are Comparative Examples.

It is clear from Table 5 that the reactors for semiconductor circuit according to the present invention have much smaller inductance change with time than the conventional Co-base amorphous alloys.

Example 17

A melt having a composition (by atomic %) of 1% Cu, 14% Si, 8% B, 5% Nb and balance substantially Fe was formed into an amorphous alloy ribbon of 5 mm in width and 20 μm in maximum thickness and 17 μm in average thickness by a single roll method. The ribbon was formed into a toroidal wound core of 6 mm in inner diameter by winding it 20 times and then heat-treated at 600°C for 1 hour in an argon gas atmosphere and then air-cooled. Thus, the magnetic core having the same alloy structure as in Example 1 was formed.

20 turns of a wire was wound around this magnetic core to provide a reactor for a semiconductor circuit. This semiconductor circuit reactor was inserted into a switching power supply in series with a diode to determine its power supply efficiency. As a result, the power supply efficiency was 80%. Also, the temperature increase of this reactor was 15°C. On the other hand, when a similar reactor made of an Fe-Si-B amorphous alloy was used, its power supply efficiency was 77%, meaning that the reactor of the present invention enjoys higher efficiency.

Example 18

Alloy melts having compositions shown in Table 6 were rapidly quenched by a single roll method to produce amorphous alloy ribbons, and each of these amorphous ribbons was formed into a toroidal core of 35 mm in outer diameter and 25 mm in inner diameter. Each wound core was heat-treated at a temperature equal to or higher than its crystallization temperature in a magnetic field of 5000 Oe in perpendicular to its magnetic path to generate extremely fine crystalline particles in the alloy structure. 10 turns of 2 wires were wound around this wound core as shown in Fig. 20 to produce a common mode choke. This common mode choke was measured with respect to DC magnetaic characteristics, a core loss $W_{2/100k}$ at 2kG, an absolute value of complex permeability at 100 kHz $|\mu|_{100k}$, effective pulse permeability μ, at a pulse width of 10 μs and ΔB of 4kG and saturation magnetostriction λs. The results are shown in Table 6.

Table 6

No.*	Composition (at%)	$B_{1.0}$ (kG)	$Br/B_{1.0}$ (%)	Hc (Oe)	$\lvert\mu\rvert_{1.0k}$	μ_e	λ_s ($\times 10^{-6}$)	$W_{1/1.0k}$ (mW/cc)
1	$Fe_{73.5}Cu_{0.5}Si_{13.5}B_9Nb_3$	12.4	18	0.014	18000	28000	+1.8	290
2	$Fe_{73}Cu_{1.5}Si_{13.5}B_9Nb_2$	12.6	8	0.012	20000	32000	+2.0	220
3	$Fe_{73}Cu_{1.5}Si_8B_9Nb_3$	14.6	14	0.058	10100	10000	+1.8	450
4	$Fe_{74.5}Cu_{1.5}Si_{13.5}B_8Nb_3$	11.6	18	0.021	21000	28000	+1.5	330
5	$Fe_{77}Cu_1Si_{10}B_9Nb_3$	14.3	25	0.024	15200	15000	+1.6	430
6	$Fe_{73.5}Cu_1Si_{13.5}B_9Ta_3$	10.5	20	0.016	21000	23000	-0.3	370
7	$Fe_{73}Cu_{1.5}Si_{13.5}B_9Mo_3$	11.2	21	0.012	22000	26000	+1.9	280
8	$Fe_{77}Cu_1Si_{13}B_9W_3$	12.1	23	0.024	18000	23000	+1.7	250
9	$Fe_{73}Cu_2Si_{13.5}B_{8.5}Hf_3$	11.6	22	0.027	20000	24000	+2.0	350
10	$Fe_{74.5}Cu_1Si_{13.5}B_9Ta_2$	12.8	20	0.019	19000	24000	+1.8	480
11	$Fe_{73}Cu_1Si_{14}B_9Zr_3$	11.7	24	0.029	18000	20000	+2.0	370
12	$Fe_{73.5}Cu_1Si_{13.5}B_9Ti_3$	11.3	25	0.037	17000	18000	+1.8	480
13	$Fe_{73}Cu_{1.5}Si_{13.5}B_9Ta_3$	11.4	22	0.018	18000	19000	+1.9	330
14	$Fe_{73}Cu_1Si_{13}B_{10}W_3$	10.0	23	0.024	17000	18000	+2.5	300
15	$Co_{69.7}Fe_{0.4}Mn_{5.5}Si_{13}B_8$ Amorphous	7.8	4	0.008	15000	2100	~0	280
16	$Fe_{73}Cu_9B_{18}$ Amorphous	15.2	21	0.10	5100	4700	+27	800
17	Mn-Zn Ferrite	5.1	19	0.18	5200	< 1000	-	500

Note*: Sample Nos. 15-17 are Comparative Examples.

Their DC magnetic characteristics are comparable to those of the Fe-base amorphous alloy, and their $|\mu|_{10\,kHz}$ was comparable to that of the Co-base amorphous alloy. In a frequency band near 100 kHz in which noise problems are most serious, the common mode chokes of the present invention have large common mode noise attenuation effects. In addition, it has been verified that the core losses at 2kG and 100kHz of the common mode chokes of the present invention were smaller than that of the Fe-base amorphous alloy, and that with respect to saturation magnetostriction, the Fe-base soft magnetic alloy is almost as small as that of the Co-base amorphous alloy.

Examole 19

An alloy melt having a composition (by atomic %) of 1% Cu, 16.5% Si, 6% B, 3% Nb and balance substantially Fe was formed into an amorphous ribbon of 7.5 mm in width and 18 μ m in thickness by a single roll method. This amorphous alloy ribbon was wound to form a toroidal core of 19.5 mm in outer diameter and 9.6 mm in inner diameter. This wound core was heat-treated in an N_2 atmosphere in a magnetic field of 3000 Oe in perpendicular to the magnetic path. In this heat treatment, it was heated at a heating rate of 10 °C/min, kept at 510 °C for 1 hour, cooled down to room temperature at a cooling rate of 2.5 °C/min.

This wound core was introduced into a phenol resin core case, and 10 turns of two wires were wound around it as shown in Fig. 20 to provide a common mode choke. Its magnetic characteristics were measured. As a result, $B_{10} = 12kG$, $B_r/B_{10} = 14\%$, $Hc = 0.018$ Oe, $\mu_{e/k} = 28000$, $|\mu|_{100k} = 22000$ and $B_1 = 11.5kG$.

Next, this common mode choke was used as a line filter in an AC 100V input line for a switching power supply operable at 50kHz. Common mode noise reading from input terminals of the power supply was measured. The results are shown in Fig. 21. It is clear from Fig. 21 that the line filter (denoted by A_9) using the common mode choke of the present invention shows larger noise level reduction effects at a lower frequency than that using a Mn-Zn ferrite core (denoted by D).

Example 20

An alloy melt (Alloy A_{10}) having a composition (by atomic %) of 1% Cu, 13.5% Si, 9% B, 3% Nb and balance substantially Fe was formed into an amorphous ribbon by a single roll method. This amorphous ribbon was wound to form a toroidal core of 31 mm in outer diameter and 18 mm in inner diameter. This wound core was heat-treated in an N_2 atmosphere by applying a magnetic field of 5000 Oe in perpendicular to its magnetic path, to generate extremely fine crystalline particles in its alloy structure.

This wound core was introduced into a Bakelite core case, and 10 turns of wires were wound around it on both primary and secondary sides to measure its magnetic characteristics; DC B-H curve and pulse permeability μ_p. The results are shown in Figs. 23 (a) and (b) respectively. It was observed from Fig. 23 (a) that the magnetic core of this Example had $B_{1C} = 12.4kG$, $B_r/B_{10} = 11\%$, $Hc = 0.011$ Oe, $\mu_{e/k} = 35000$ and a core loss $W_{2/100k} = 230mW/cc$. For comparison, those of Mn-Zn ferrite (D) and Co-base amorphous alloy ($Co_{69.7}Fe_{0.4}Mn_{5.9}Si_{15}B_9$, Alloy B_4) are also shown in Fig. 23 (b).

It has been verified that the magnetic core of the present invention shows high saturation magnetic flux density and permeability with no variation with time and low squareness ratio and core loss, and that accordingly it is superior to those of comparative examples in the dependency of effective pulse permeability on magnetic flux density variation ΔB. Therefore, when used as common mode choke, it is less likely to be saturated by high-voltage noises, keeping high inductance. Thus, it can provide a line filter having excellent high-voltage pulse attenuation characteristics. In addition, the frequency characteristics of an absolute value of complex permeability $|\mu|$ of this magnetic core was measured. The results are shown in Fig. 24. In Fig. 24, A_{11} denotes the $Fe_{73.5}Cu_1Nb_3Si_{13.5}B_9$ alloy of the present invention, B_5 denotes the $Co_{70.7}Fe_{0.3}Mn_5Si_{15}B_9$ amorphous alloy (comparative example), C_5 denotes the $Fe_{77.5}Si_9B_{13.5}$ amorphous alloy (comparative example), and D denotes Mn-Zn ferrite. The fact that A_{11} has large $|\mu|$ means that it has large attenuation effects to usual noises. The magnetic core of the present invention has $|\mu|$ comparable to or even higher than that of the Co-base amorphpous alloy. Accordingly, when it is used for a transformer core, it can reduce transformer's exciting current and is less saturated at highΔB, and if temperature increase does not cause serious problems, it can be miniaturized. Therefore, high efficiency transformer can be obtained from it.

Example 21

An alloy melt having a composition (by atomic %) of 1% Cu, 13.5% Si, 7.2% B, 2.5% Nb and balance substantially Fe was formed into an amorphous ribbon of 6.5 mm in width by a single roll method. This amorphous ribbon was wound to form a toroidal core of 20 mm in outer diameter and 10 mm in inner diameter. This wound core was heat-treated under the following conditions:

(a) Heating at 550°C for 1 hour in an Ar atmosphere without magnetic field, and

(b) Heating at 550°C for 1 hour in the same atmosphere as in (a) while applying a magnetic field of 3000 Oe in perpendicular to its magnetic path. 12 turns of two wires were wound around each wound core to provide a common mode choke. Each common mode choke was measured with respect to pulse attenuation characteristics by using a circuit shown in Fig. 26 (a), in which 25 denotes an impulse noise simulator, 26 a sample and 27 an oscilloscope. The measured pulse attenuation characteristics are shown in Fig. 26 (b), in which A_{12} denotes the common mode choke produced from the magnetic core heat-treated by (a), and A_{13} that produced from the magnetic core heat-treated by (b). Fig. 26 (b) also shows the pulse attenuation characteristics of common mode chokes made of Mn-Zn ferrite (D) and Fe-base amorphous alloy (C_6). It has been verified that even the common mode choke A_{12} heat-treated without magnetic field shows higher pulse attenuation characteristics than the Mn-Zn ferrite D, and that the common mode choke A_{13} heat-treated in a magnetic field show higher pulse attenuation characteristics than the Fe-base amorphous alloy C_6.

Example 22

With respect to the common mode chokes produced in Example 21, the dependency of attenuation on frequency was measured. A measuring circuit used is shown in Fig. 27 (a), in which 28 denotes a standard signal generator, 29 a selective level meter, 30 a sample, and 31 a power divider. Input signal level was 0 dbm. The results are shown in Fig. 27 (b) together with those of Mn-Zn ferrite D. It has been verified that the common mode choke of the present invention shows better attenuation effects than that of the Mn-Zn ferrite D in all frequency area.

Example 23

With respect to common mode chokes using the finely crystallized alloys of the present invention and those using conventional alloys, magnetic characteristics and high-voltage pulse characteristics are shown in Table 7. Here, each common mode choke comprises a wound core of 12.5 mm in width, 25 mm in outer diameter and 15 mm in inner diameter and 22 turns of 2 wires. Incidentally, a magnetic field, if necessary, was applied at 3000 Oe in perpendicular to the magnetic path during heat treatment.

Table 7

No.*	Composition (at%)	Bs (G)	Output Voltage Vo (V)	$\lvert\mu\rvert_{1,000}$	Magnetic Field in Heat Treatment
1	$(Fe_{0.94}Co_{0.06})_{73.5}Cu_1Si_{13.5}B_9Nb_3$	13000	15	18000	Yes
2	$Fe_{73.5}Cu_1Si_{22.5}B_5Nb_3$	10800	16	17000	Yes
3	$(Fe_{0.7}Co_{0.3})_{73.5}Cu_1Si_{13.5}B_9Nb_3$	12300	14	10500	No
4	$Fe_{73.5}Cu_1Si_{13.5}B_9Nb_3$	13300	15	19000	Yes
5	$(Fe_{0.94}Ni_{0.06})_{73.5}Cu_1Si_{13.5}B_9Nb_3$	12300	17	17000	Yes
6	$Fe_{73}Cu_1Si_{13}B_9Nb_3$	11400	14	20000	Yes
7	$(Fe_{0.92}Co_{0.08})_{73.5}Cu_1Si_{13.5}B_9Nb_3$	12700	12	6000	No
8	$Fe_{73}Cu_1Si_{13}B_9Nb_3$	14200	15	18000	Yes
9	$Fe_{80}Si_{10}B_{10}$ (40% Amorphous)**	16500	20	1800	No
10	$Fe_{80}Si_{10}B_{10}$ (20% Amorphous)**	16500	50	900	No

Note *: Sample Nos. 9 and 10 are Comparative Examples.

**: Balance crystalline

The common mode chokes of the present invention show higher absolute values of | μ | at 100 kHz and better noise attenuation characteristics than those made from the conventional amorphous alloys which were partially crystallized. Also, since they show small output voltage V_0 to pulse voltage of 1000 V and 1μ sec, excellent line filters can be produced by using the common mode chokes of the present invention. In addition, it has been confirmed that | μ | can be improved by heat treatment in a magnetic field.

Example 24

Table 8 shows magnetic characteristics and high-voltage pulse characteristics of the common mode chokes of thepresent invention having the structure of Example 23. Incidentally, a magnetic field of 3000 Oe was applied in perpendicular to the magnetic path during heat treatment. In addition, as in Example 23, an absolute value of complex permeability | μ | at 100 kHz and output voltage V_0 to pulse voltage of 1000 V and 1μ sec when combined in a line filter were measured for each common mode choke. The results are also shown in Table 8.

Table 8

No.	Composition (at%)	Vo (V)	|μ|max	W2/100k (mW/cc)
1	$Fe_{71}Cu_1Si_{15}B_9Nb_3Ti_1$	17	18400	240
2	$Fe_{69}Cu_1Si_{15}B_9W_5V_1$	16	19200	270
3	$Fe_{69}Cu_1Si_{16}B_8Mo_5Mn_1$	18	18000	270
4	$Fe_{69}Cu_1Si_{17}B_7Nb_5Ru_1$	19	17000	260
5	$Fe_{71}Cu_1Si_{14}B_{10}Ta_3Rh_1$	17	16500	300
6	$Fe_{72}Cu_1Si_{14}B_9Zr_3Pd_1$	15	17000	320
7	$Fe_{72.5}Cu_{0.5}Si_{14}B_9Hf_3Ir_1$	16	18500	330
8	$Fe_{70}Cu_2Si_{16}B_9Nb_3Pt_1$	16	19100	260
9	$Fe_{70.5}Cu_{1.5}Si_{15}B_9Nb_3Au_1$	14	19000	250
10	$Fe_{71.5}Cu_{0.5}Si_{15}B_9Nb_3Zn_1$	18	15200	310
11	$Fe_{69.5}Cu_{1.5}Si_{15}B_9Nb_3Mo_1Sn_1$	17	17000	270
12	$Fe_{69.5}Cu_{2.5}Si_{15}B_9Nb_3Ta_1Re_1$	17	17100	310
13	$Fe_{70}Cu_1Si_{15}B_9Nb_3Zr_1Al_1$	19	18000	300
14	$Fe_{70}Cu_1Si_{15}B_9Nb_3Hf_1Sc_1$	17	17800	290
15	$Fe_{70}Cu_1Si_{15}B_9Hf_3Zr_1Y_1$	18	16400	330
16	$Fe_{71}Cu_1Si_{15}B_9Nb_3La_1$	16	15000	390
17	$Fe_{69.7}Cu_1Si_{17}B_9Mo_5Ce_1$	17	13200	380
18	$Fe_{69.7}Cu_1Si_{17}B_9W_5Pr_1$	17	12800	400
19	$Fe_{69.7}Cu_1Si_{17}B_9Ta_3Nb_1$	18	13600	410
20	$Fe_{69.7}Cu_1Si_{17}B_9Zr_3Sm_1$	16	11000	370
21	$Fe_{69.7}Cu_1Si_{15}B_{10}Hf_3Eu_1$	14	11200	380
22	$Fe_{69.8}Cu_1Si_{16}B_9Nb_3Gd_1$	16	11100	390
23	$Fe_{69.8}Cu_1Si_{19}B_8Nb_3Tb_1$	18	11000	360
24	$Fe_{71.2}Cu_1Si_{14}B_9Nb_3Dy_1$	19	10800	370
25	$Fe_{71.2}Cu_1Si_{14}B_9Nb_3Ho_1$	19	10100	360
26	$Fe_{71}Cu_1Si_{14}B_9Nb_3Cr_1Ti_1$	18	17200	240
27	$(Fe_{0.95}Co_{0.05})_{71.2}Cu_1Si_{14}B_9Nb_3Cr_1$	17	16800	230
28	$(Fe_{0.95}Co_{0.05})_{71.2}Cu_1Si_{14}B_9Ta_3Ru_1$	19	15800	270

Table 8 (continued)

No.	Composition (at%)	Vo (V)	$\|\mu\|_{100k}$	$W_{2/100k}$ (mW/cc)
29	$(Fe_{0.8}Co_{0.1})_{72}Cu_1Si_{13}B_9Ta_3Mn_1$	19	15500	280
30	$(Fe_{0.89}Ni_{0.01})_{72}Cu_1Si_{14}B_9Ta_3Ru_1$	18	14800	270
31	$(Fe_{0.85}Ni_{0.05})_{71}Cu_1Si_{14}B_9Ta_3Cr_1Ru_1$	19	14300	270
32	$(Fe_{0.90}Ni_{0.1})_{68}Cu_1Si_{15}B_9W_5Ti_1Ru_1$	19	13900	300
33	$(Fe_{0.88}Co_{0.03}Ni_{0.02})_{68.5}Cu_1Si_{15.5}B_9W_5Cr_1Rh_1$	18	14200	270
34	$(Fe_{0.88}Co_{0.01}Ni_{0.01})_{69}Cu_1Si_{15}B_9W_5Ru_3$	19	14300	240
35	$Fe_{73}Cu_1Si_{13}B_9Nb_3C_1$	18	17200	230
36	$Fe_{73}Cu_1Si_{13}B_9Nb_3Ge_1$	15	17300	220
37	$Fe_{73}Cu_1Si_{13}B_9Nb_3P_1$	14	13200	240
38	$Fe_{73}Cu_1Si_{13}B_9Nb_3Ga_1$	16	13800	250
39	$Fe_{73}Cu_1Si_{13}B_9Nb_3Sb_1$	17	15800	290
40	$Fe_{73}Cu_1Si_{13}B_9Nb_3As_1$	16	13200	310
41	$Fe_{71}Cu_1Si_{13}B_9Mo_5C_2$	19	15900	330
42	$Fe_{70}Cu_1Si_{14}B_6Mo_3Cr_1C_5$	19	11000	330
43	$(Fe_{0.85}Co_{0.05})_{70}Cu_1Si_{13}B_9Nb_5Al_1C_1$	18	14500	340
44	$(Fe_{0.88}Ni_{0.02})_{70}Cu_1Si_{13}B_9W_5V_1Ge_1$	17	17800	340
45	$Fe_{80.5}Cu_{1.5}Si_{13}B_9Nb_5Ru_1C_2$	17	16900	270
46	$Fe_{73}Cu_1Si_{14}B_9Ta_3Cr_1Ru_2C_1$	16	17800	290
47	$Fe_{73}Cu_1Si_{14}B_9Nb_5Be_1$	18	16200	260
48	$Fe_{80}Cu_1Si_{15}B_9Nb_5Mn_1Be_1$	17	15800	260
49	$Fe_{80}Cu_2Si_{16}B_8Zr_5Rh_1In_1$	16	16100	270
50	$Fe_{71}Cu_2Si_{13}B_7Hf_5Au_1C_1$	15	15800	280
51	$Fe_{80}Cu_1Si_{16}B_{10}Mo_5Sc_1Ge_1$	19	14300	280
52	$Fe_{87.5}Cu_{0.5}Si_{16}B_{11}Nb_5Y_1P_1$	18	14200	260
53	$Fe_{87}Cu_1Si_{13}B_{15}Nb_5La_1Ga_1$	17	13200	400
54	$(Fe_{0.85}Ni_{0.05})_{70}Cu_1Si_{13}B_9Nb_5Sm_1Sb_1$	18	16800	420
55	$(Fe_{0.82}Co_{0.08})_{70}Cu_1Si_{13}B_9Nb_5Zn_1As_1$	17	15900	390
56	$(Fe_{0.86}Ni_{0.02}Co_{0.02})_{70}Cu_1Si_{13}B_9Nb_5Sn_1In_1$	18	16700	390

Table 8 (continued)

No.	Composition (at%)	Vo (V)	$\|\mu\|_{100k}$	$W_{2/100k}$ (mW/cc)
57	$Fe_{85}Cu_1Si_{13}B_9Mo_3Re_1C_2$	17	15300	340
58	$Fe_{85}Cu_1Si_{13}B_9Mo_3Ce_1C_2$	16	13300	400
59	$Fe_{85}Cu_1Si_{13}B_9W_3Pr_1C_2$	14	14300	410
60	$Fe_{85}Cu_1Si_{13}B_9W_3Nd_1C_2$	15	15000	380
61	$Fe_{85}Cu_1Si_{14}B_9Ta_3Gd_1C_2$	18	13200	410
62	$Fe_{85}Cu_1Si_{13}B_9Nb_3Tb_1C_2$	9	11000	420
63	$Fe_{78}Cu_1Si_{14}B_8Nb_3Dy_1Ge_1$	9	10000	410
64	$Fe_{78}Cu_1Si_{13}B_7Nb_3Pd_1Ge_1$	18	15000	410
65	$Fe_{78}Cu_1Si_{13}B_9Nb_3Ir_1P_1$	17	13800	410
66	$Fe_{78}Cu_1Si_{13}B_9Nb_3Os_1Ga_1$	19	15100	270
67	$Fe_{71}Cu_1Si_{14}B_9Ta_3Cr_1C_1$	15	14800	280
68	$Fe_{87}Cu_1Si_{15}B_6Zr_5V_1C_5$	18	13700	300
69	$Fe_{85}Cu_1Si_{16}B_5Hf_5Cr_2C_6$	17	13800	280
70	$Fe_{85}Cu_1Si_{14}B_9Mo_6Ru_3C_1$	15	15800	270
71	$Fe_{78}Cu_1Si_{14}B_9Mo_3Ti_1Ru_1C_1$	15	13800	270
72	$Fe_{87}Cu_1Si_{14}B_9Nd_6Rh_2C_1$	16	15000	250

Example 25

An amorphous alloy ribbon having the same composition as in Example 19 and having a width of 7.5 mm and a thickness of 20μ m was formed into a toroidal core as shown in Fig. 22 (a), and the toroidal core was heat-treated while applying a magnetic field of 5000 Oe in perpendicular to its magnetic path during the overall period of heat treatment, to generate fine crystalline particles in the alloy structure. Incidentally, the heat treatment was conducted by heating to 500°C at a heating rate of 20°C/min, keeping at 500°C for 1 hour, cooling to 280°C at a cooling rate of 5°C/min, keeping at 280°C for 2 hours, and then cooling to room temperature at a cooling rate of 2°C/min. A Capton tape was wound around this wound core as shown in Fig. 22 (b) to provide a transformer core. After winding wires around this core, its magnetic characteristics were measured. As a result, B_{10} = 12kG, B_r/B_{10} = 12%, Hc = 0.012 Oe and $W_{2/100k}$ = 240mW/cc. In addition, when a transformer core was produced by first impregnating the wound core with an epoxy resin in vacuum to provide a molded core and then winding a Capton tape around the molded core, the transformer core showed B_{10} = 12kG, B_r/B_{10} = 18%, Hc = 0.018 Oe and $W_{2/100k}$ = 370 mW/cc.

For comparison, an amorphous alloy ribbon consisting essentially of 13.5% Si, 9% B, 3% Nb and balance substantially Fe by atomic % was formed into a toroidal core, and a Capton tape was wound around it to produce a transformer core (Comparative Example 1), and the above toroidal core was

impregnated with an epoxy resin and then a Capton tape was wound around it to provide a transformer core (Comparative Example 2). The transformer core of the comparative example 1 showed a core loss $W_{2/100k}$ = 1500 mW/cc, while that of comparative example 2 showed extremely large core loss $W_{2/100k}$ = 3300 mW/cc. Thus, the transformer core of the present invention shows much smaller core loss even though it is impregnated with a resin.

Example 26

The finely crystallized alloy having the composition as in Example 20 was formed into an E core shown in Fig. 25 (a), and heat-treated at 550 °C for 1 hour in an Ar atmosphere to generate extremely fine crystalline particles in its alloy structure. And then an E-type transformer core was formed as shown in Fig. 25 (b). A measurement of the magnetic characteristics of this core shows that its saturation magnetic flux density was 12.6kG, more than double that of Mn-Zn ferrite and its core loss $W_{2/100k}$ was 280 mW/cc.

13 turns of a wire on a primary side and 6 turns of a wire on a secondary side were wound around this core, and mounted as a transformer in a switching power supply operable at 200kHz. Temperature increase Δ T of the core was measured. The results are shown in Table 9.

Table 9

Magnetic Core	Δ T (°C)
$Fe_{74.5}Cu_1Si_{13.5}B_9Nb_2$	30
Mn-Zn ferrite	38

It shows that the core of the present invention suffers from less temperature increase than that of Mn-Zn ferrite, exerting less influence to other elements.

Example 27

An alloy melt of $Fe_{73.5}Cu_1Si_{16.5}B_6Nb_3$ (by atomic %) was formed into an amorphous alloy ribbon, and the amorphous alloy ribbon was coated with an MgO layer by an electrophoresis method. It was then wound in the form shown in Fig. 28 (a), and heat-treated at 530 °C for 1 hour and then cooled. After heat treatment, this core was impregnated with varnish and cut at center by a peripheral slicer. The cut portions were ground and lapped to produce a cut core shown in Fig. 28 (b). Its core loss at 100 kHz and 2kG was as low as 500 mW/cc.

Such cut core can be formed into a transformer by inserting the bobbin provided with wires into the cut core. Accordingly, it is advantageous in that its winding operation is easy. Also, by providing a gap, the core's effective permeability can be controlled.

Example 28

Fig. 29 shows dependency of a core loss on frequency of the magnetic core of $Fe_{73.5}Cu_1Si_{13.5}B_9Nb_3$ - (Alloy A_{16}, present invention) as shown in Example 14, together with those of the conventional materials. B_6 denotes a $Co_{69.7}Fe_{0.4}Mn_{5.8}Si_{15}B_9$ amorphous alloy, C_7 denotes an $Fe_{76.5}Cr_1Si_{13.5}B_9$ amorphous alloy, and D denotes Mn-Zn ferrite. The magnetic core of the present invention showed a core loss which was equal to or smaller than that of the Co-base amorphous alloy (B_6) up to a high-frequency region and much smaller than those of the Fe-base amorphous alloy (C_7) and the Mn-Zn ferrite (D). Thus, the magnetic core of the present invention is excellent as a transformer operable at high frequency. With respect to a saturation magnetic flux density, the magnetic core of the present invention is much higher than those of the Mn-Zn ferrite and the Co-base amorphous alloy, meaning that the magnetic core of the present invention can be used for miniaturized transformers.

Claims

1. A magnetic core made of an Fe-base soft magnetic alloy consisting essentially of Fe, Cu and M wherein M is at least one of the elements Nb, W, Ta, Zr, Hf, Ti and Mo, at least 50% of the alloy structure being occupied by fine crystalline particles, and the change ratio X of the effective permeability with time of said magnetic core being 0.3 or less, where X is defined by the following formula:

$X = 1 - \mu_b \quad \mu_a$

wherein μ_a is the effective permeability at 1 kHz, and μ_b is the effective permeability at 1kHz after heating at 100 °C for 1000 hours in the air.

2. The magnetic core according to claim 1, wherein said Fe-base soft magnetic alloy has a saturation magnetic flux density Bs of 1T or more and an effective permeability μ_{ek} of 5×10^3 or more.

3. The magnetic core according to claim 1 or 2, wherein said Fe-base soft magnetic alloy has saturation magnetostriction λ_s of $+5 \times 10^{-6} - -5 \times 10^{-6}$.

4. The magnetic core according to any one of claims 1 to 3, having a DC B-H curve's squareness ratio $B_r \quad B_{\cdot 3}$ of 30% or less, an absolute value of complex permeability $|\mu|$ at 100 kHz of 1000 or more, a magnetic flux density B_1 at 1 Oe (80 A/m) of 0.5 T or more and a magnetic flux density $B_{1 3}$ at 10 Oe (800 A/m) of 1 T or more.

5. A saturable reactor comprising the magnetic core according to any one of claims 1 to 4.

6. The saturable reactor according to claim 5, wherein its uncontrollable magnetic flux density ΔB_b at 50 kHz is 0.3 T or less.

7. A reactor for a semiconductor circuit comprising the magnetic core according to any one of claims 1 to 4.

8. The reactor for a semiconductor circuit according to any one of claims 5 to 7, wherein said Fe-base soft magnetic alloy has a DC B-H curve's squareness ratio $B_r : B_{1 3}$ of 70% or more.

9. A common mode choke comprising the magnetic core according to any one of claims 1 to 4.

10. A line filter containing the common mode choke of claim 9.

11. A high-frequency transformer core comprising the magnetic core according to any one of claims 1 to 4.

12. A high-frequency transformer comprising the magnetic core of claim 11 and two or more windings.

13. A method of producing a magnetic core comprising the steps of rapidly quenching an alloy melt consisting essentially of Fe, Cu and M, wherein M is at least one of the elements Nb, W, Ta, Zr, Hf, Ti and Mo to form an amorphous ribbon, forming said amorphous ribbon into a wound core and then heat-treating said wound core so that said alloy has fine crystalline particles occupying at least 50% of its structure.

FIG. 1

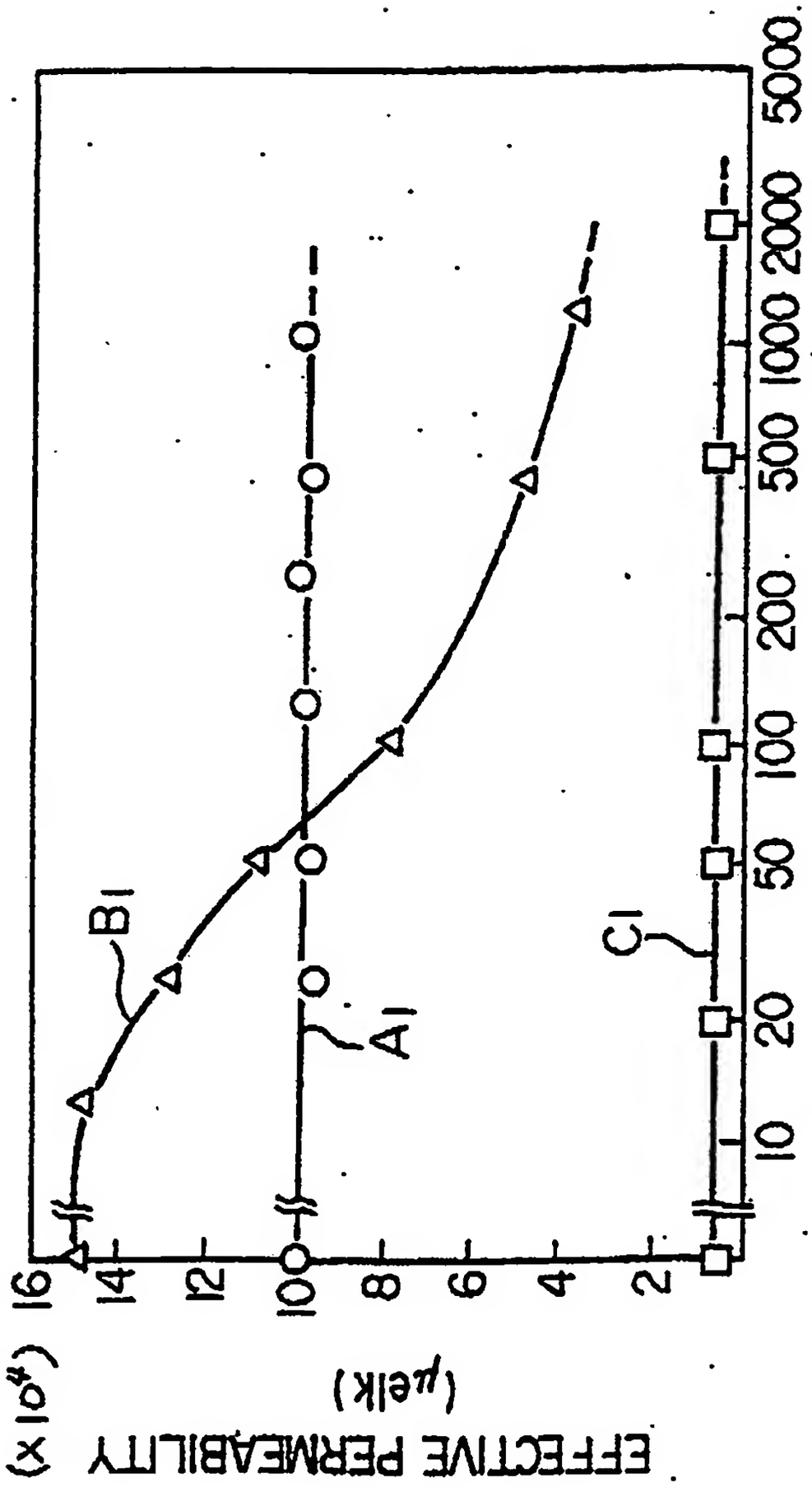
EFFECTIVE PERMEABILITY (μeik)
(×10⁻³)
16
14
12
10
8
6
4
2
B1
A1
C1
TIME (hr)
10
20
50
100
200
500
1000
2000
5000

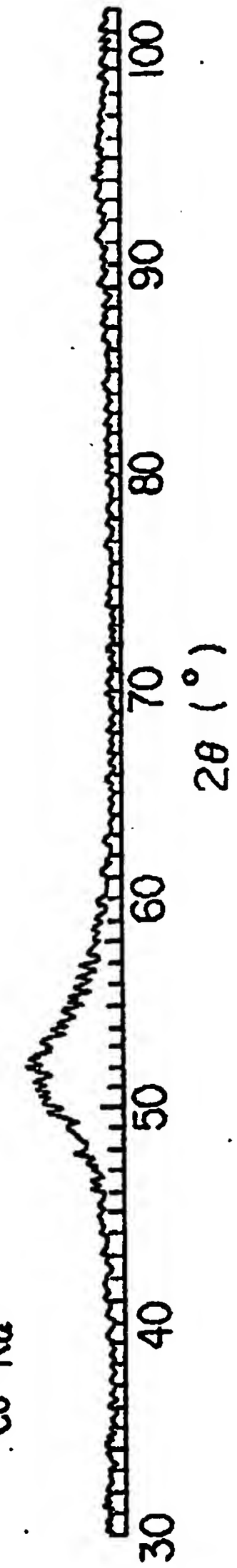
Co Kα
30
40
50
60
70
80
90
100
2θ (°)

FIG. 2

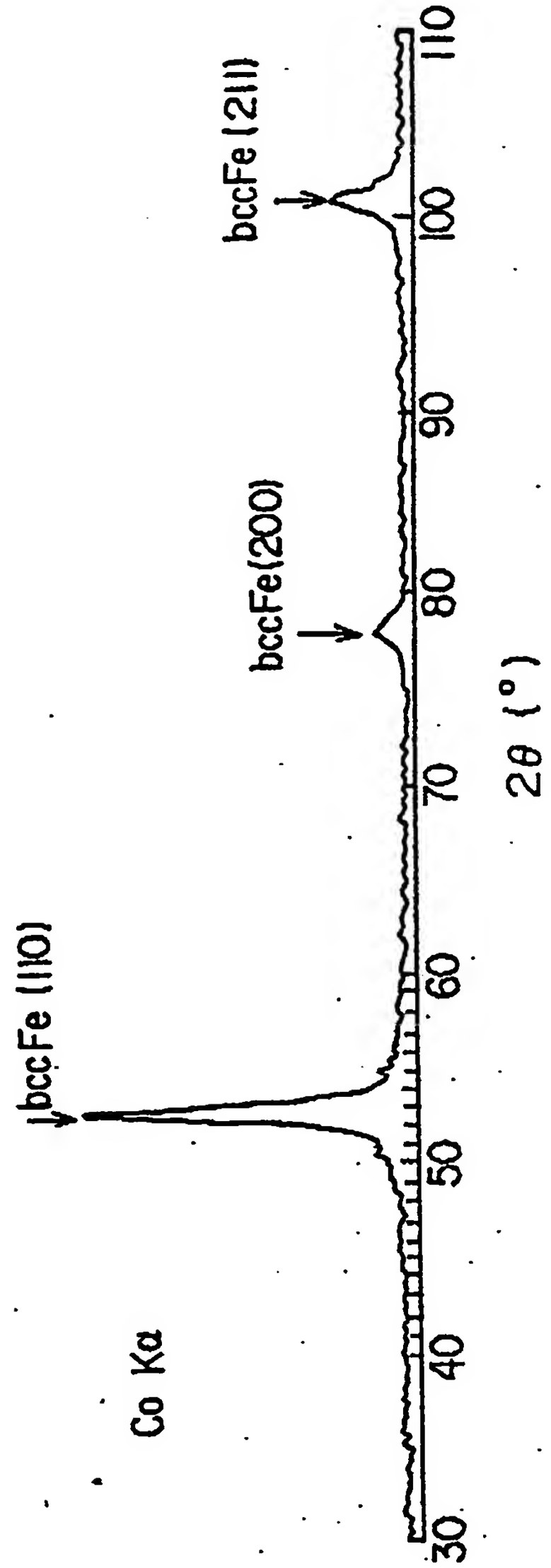
Co Kα
bccFe (110)
bccFe(200)
bccFe (211)
30
40
50
60
70
80
90
100
110
2θ (°)

FIG. 3(a)

FIG. 3 (b)

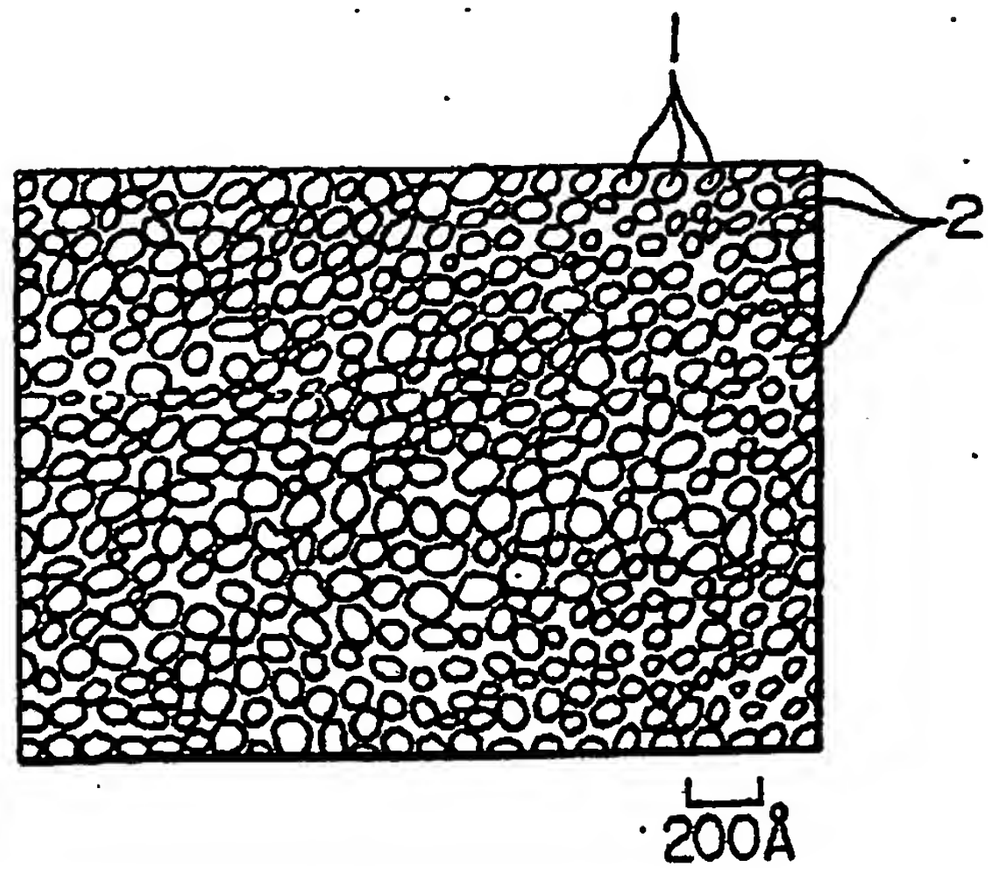

FIG. 5

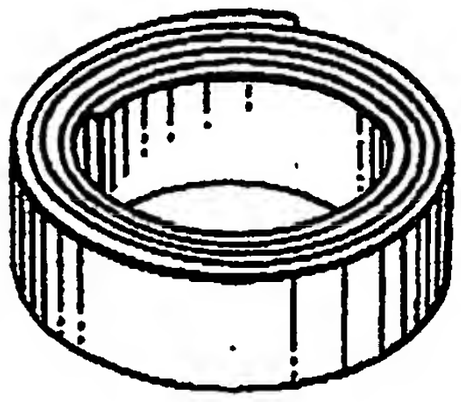

FIG. 4

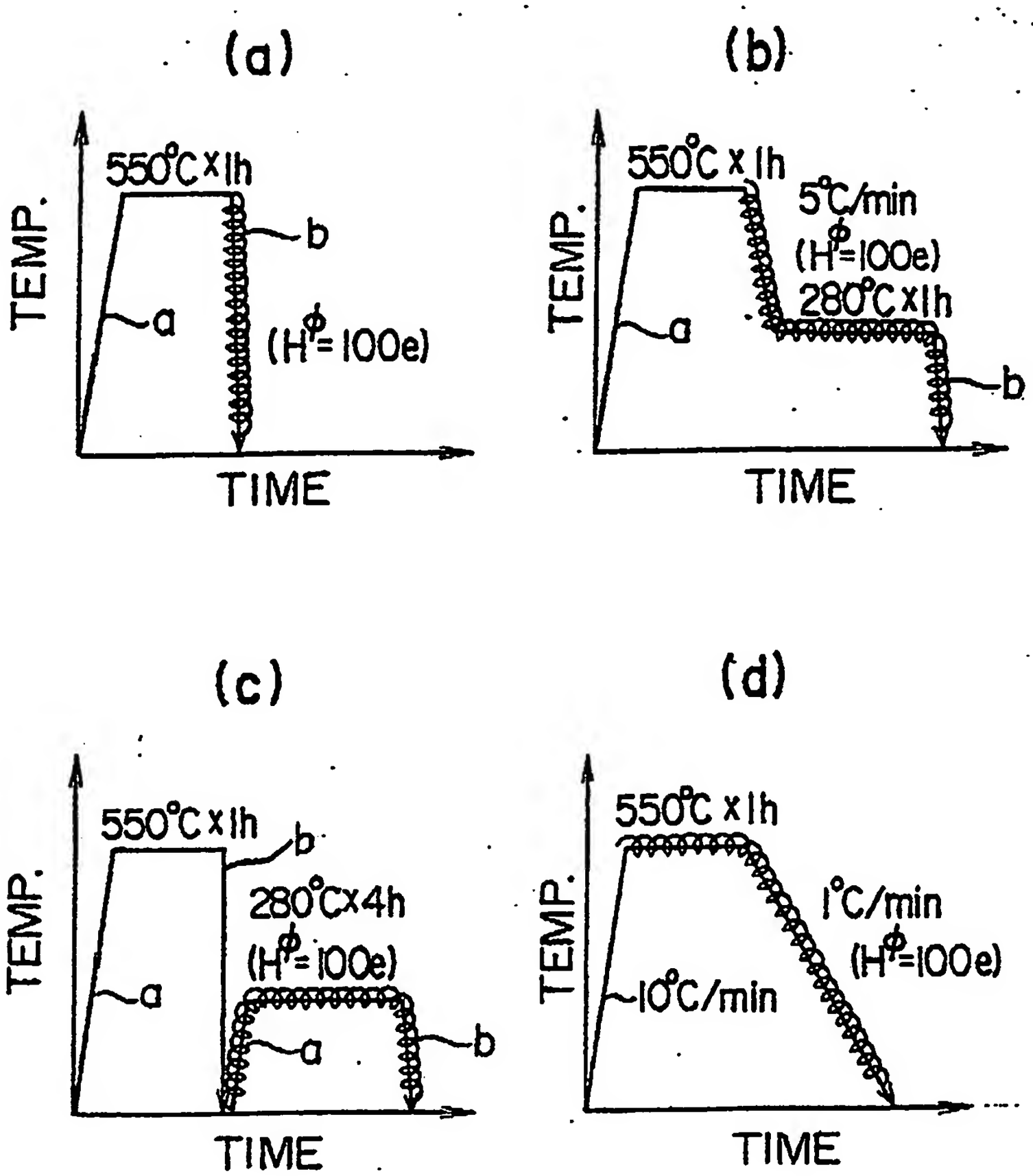

FIG. 4

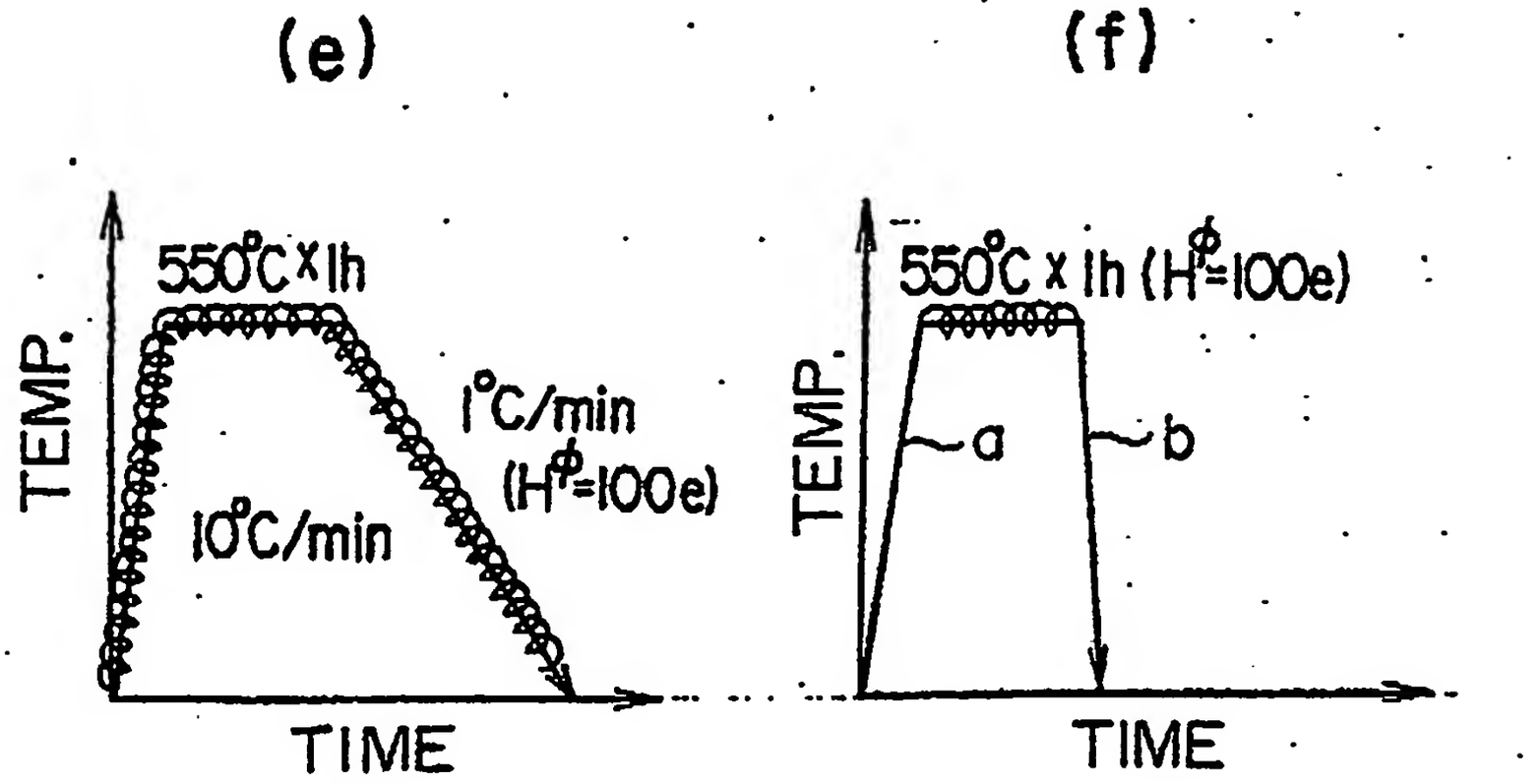
(e)
550°C x 1h
1°C/min
(H$^{\phi}$=100e)
10°C/min
TEMP.
TIME
(f)
550°C x 1h (H$^{\phi}$=100e)
a
b
TEMP.
TIME

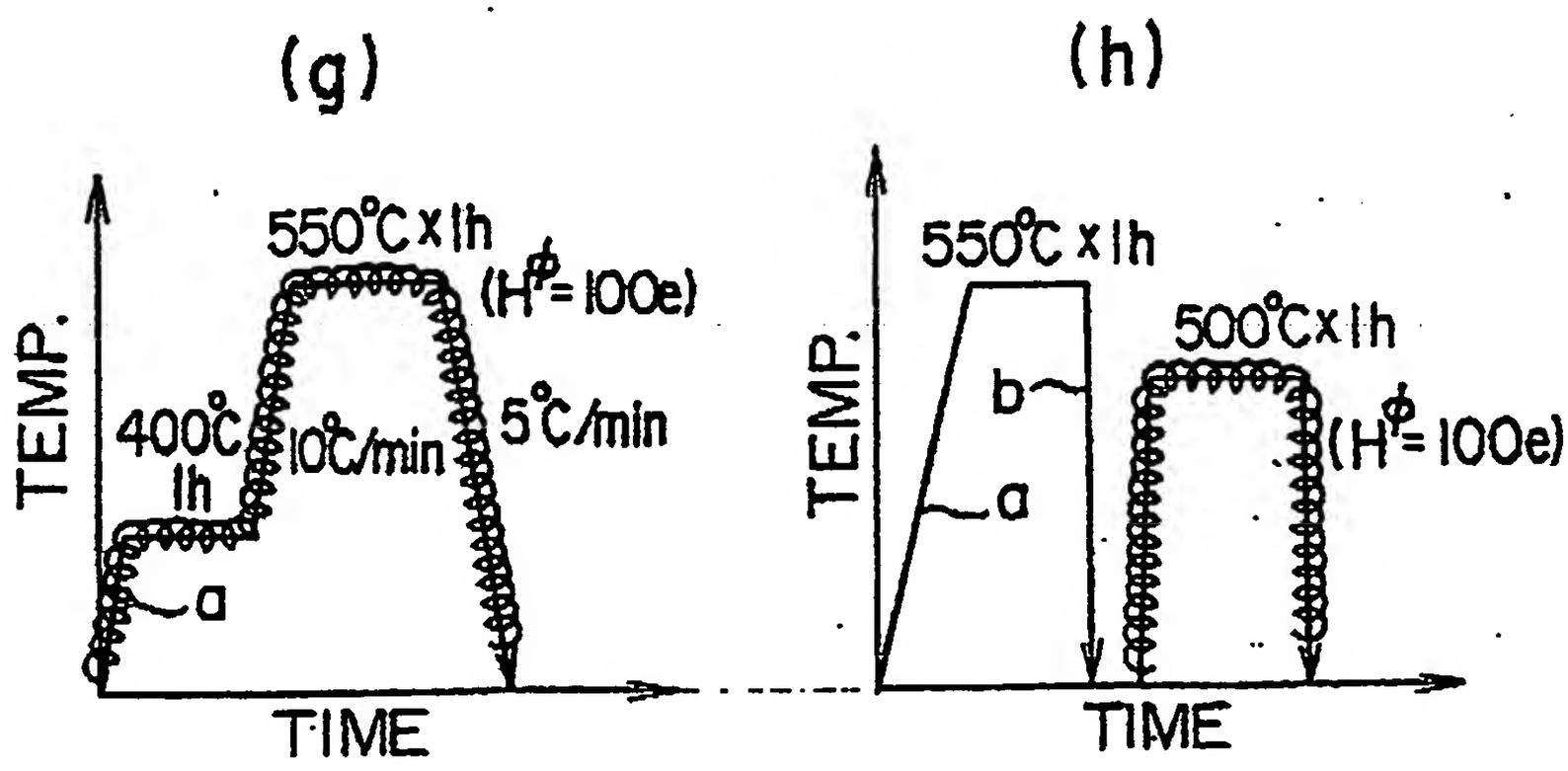
(g)
550°C x 1h
(H$^{\phi}$=100e)
400°C
1h
10°C/min
5°C/min
a
TEMP.
TIME
(h)
550°C x 1h
500°C x 1h
(H$^{\phi}$=100e)
b
a
TEMP.
TIME

FIG. 6

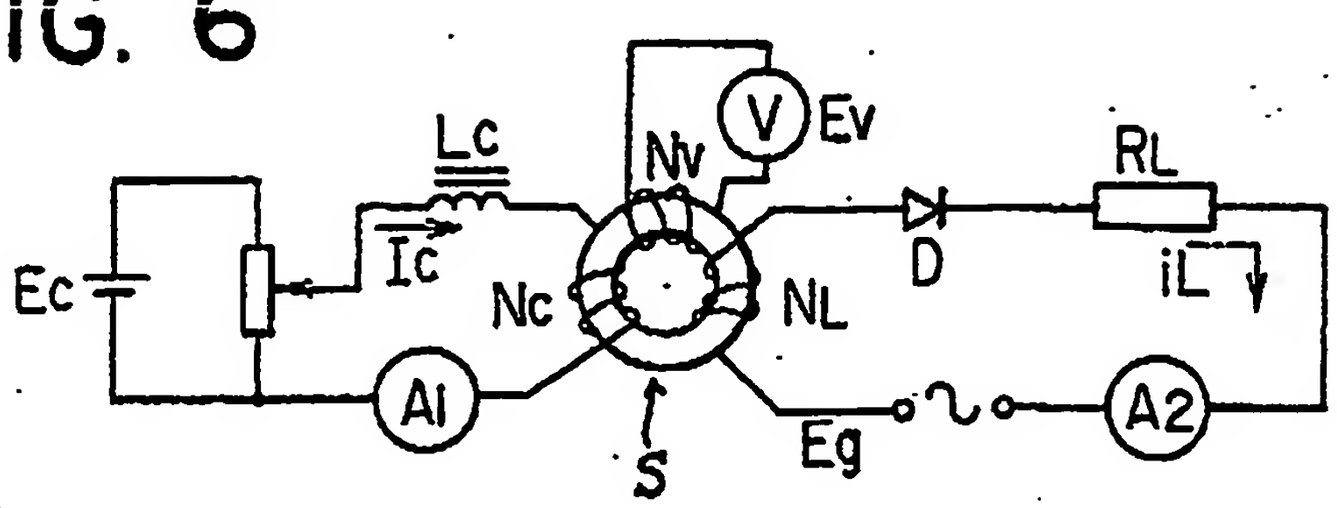

FIG. 7

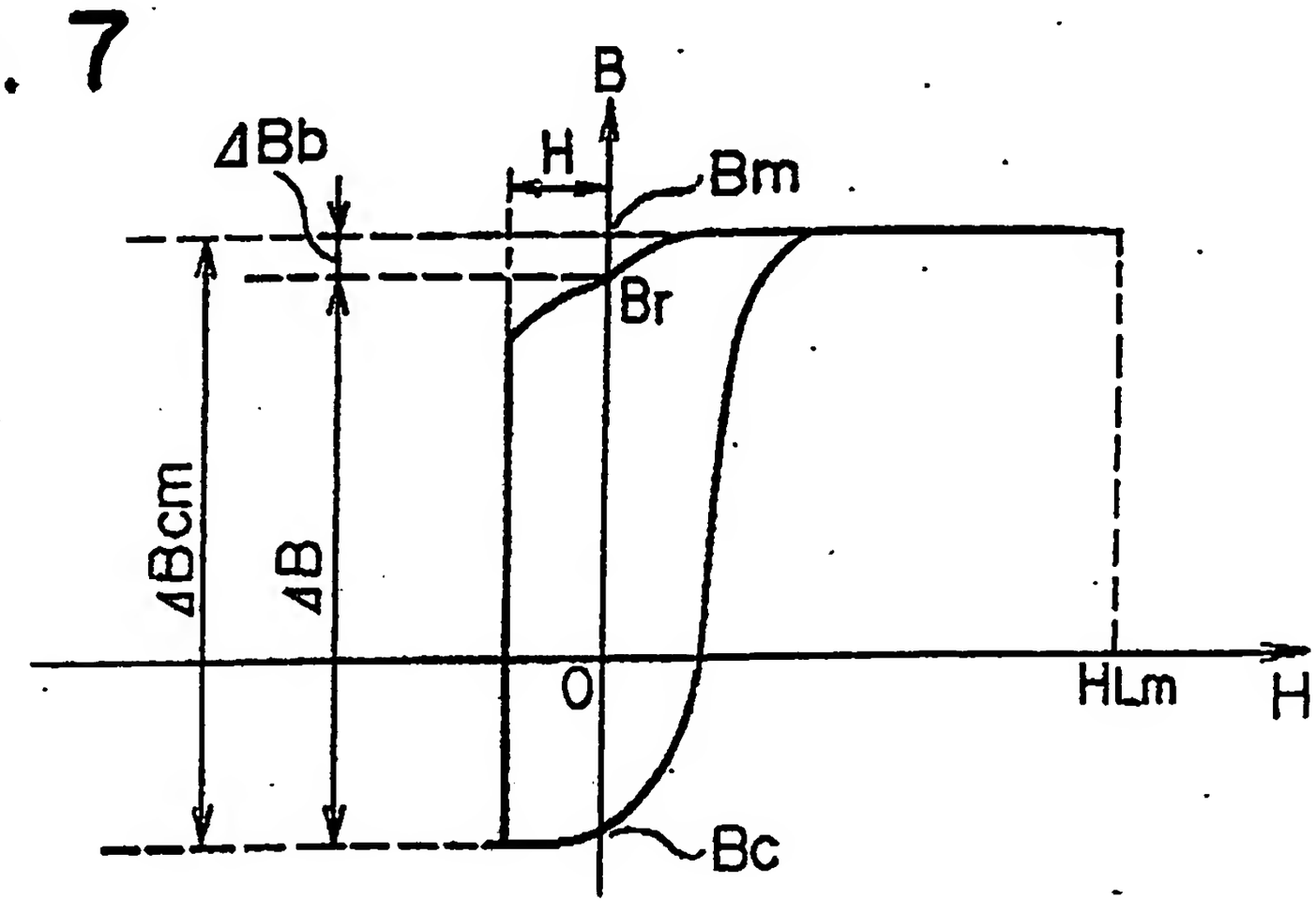

FIG. 8

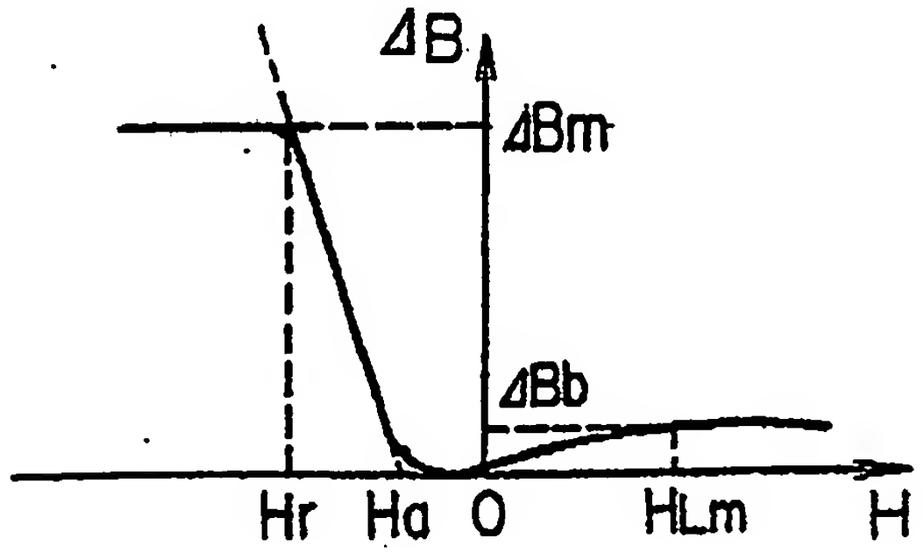

FIG. 9

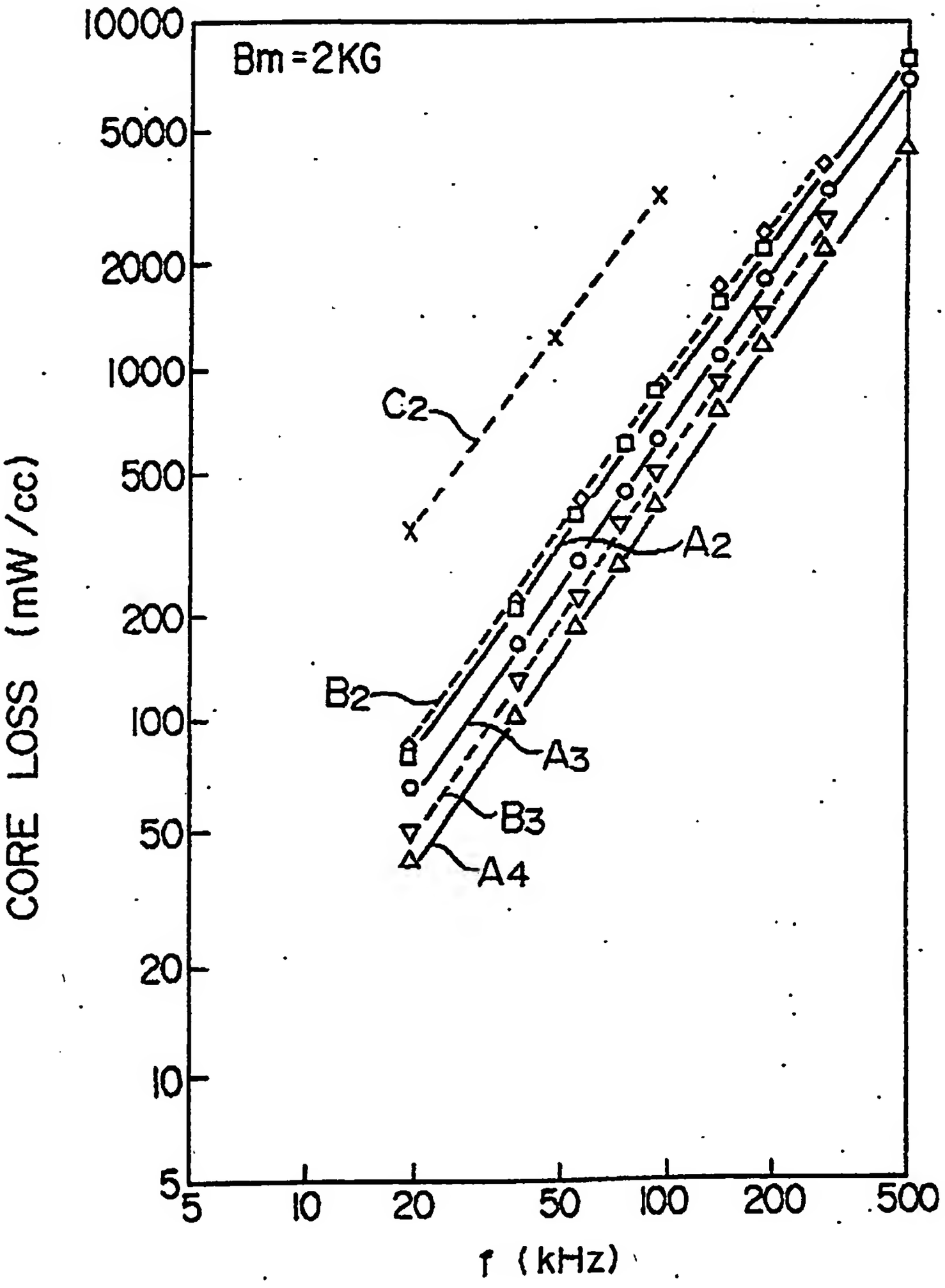
Bm=2KG
10000
5000
2000
1000
500
200
100
50
20
10
5
CORE LOSS (mW/cc)
C2
A2
B2
A3
B3
A4
5
10
20
50
100
200
500
f (kHz)

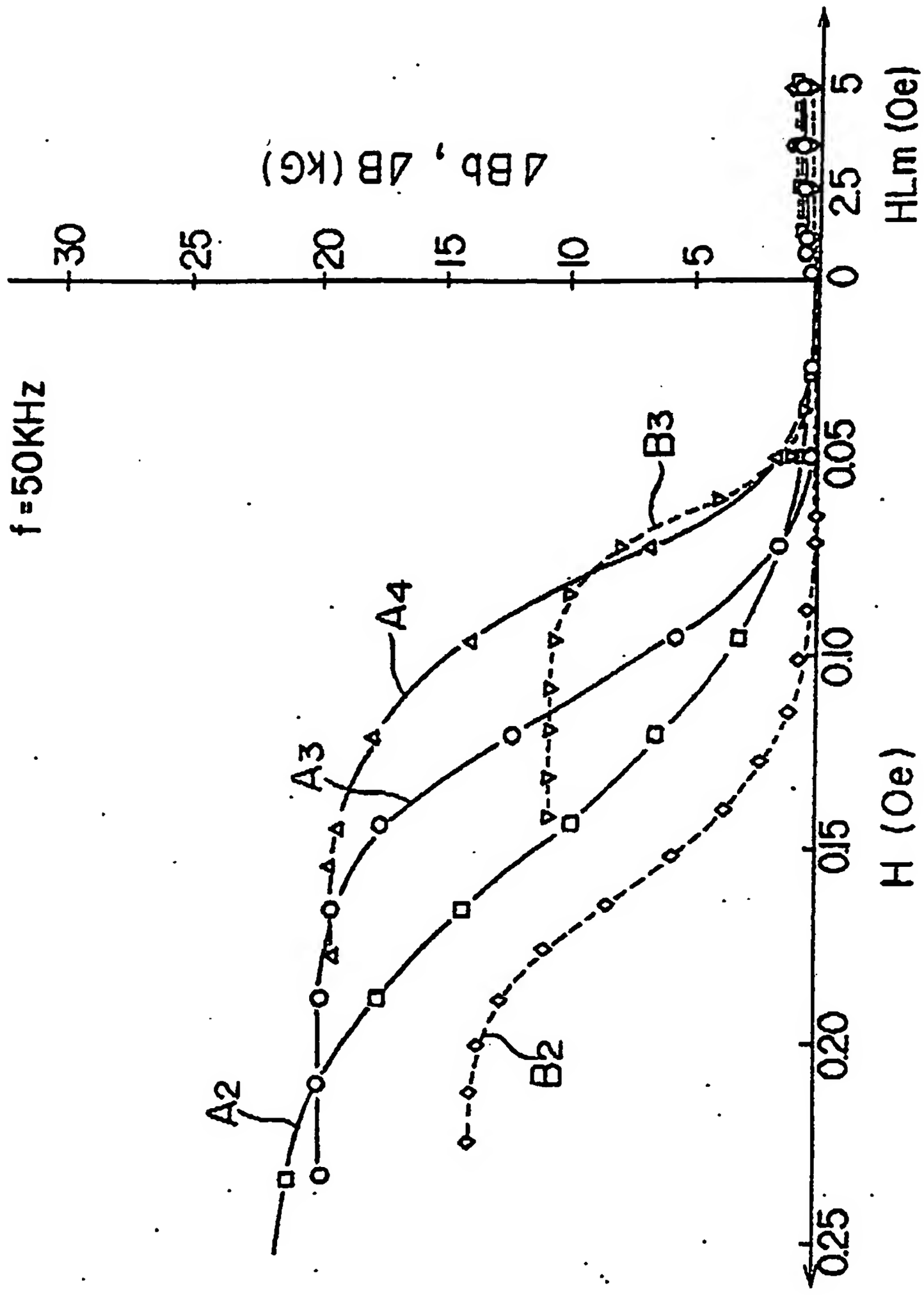
f=50KHz
ΔBb , ΔB (KG)
30
25
20
15
10
5
0
25
5
HLm (Oe)
A2
A3
A4
B2
B3
0.05
0.10
0.15
0.20
0.25
H (Oe)

FIG. 10

FIG. 11

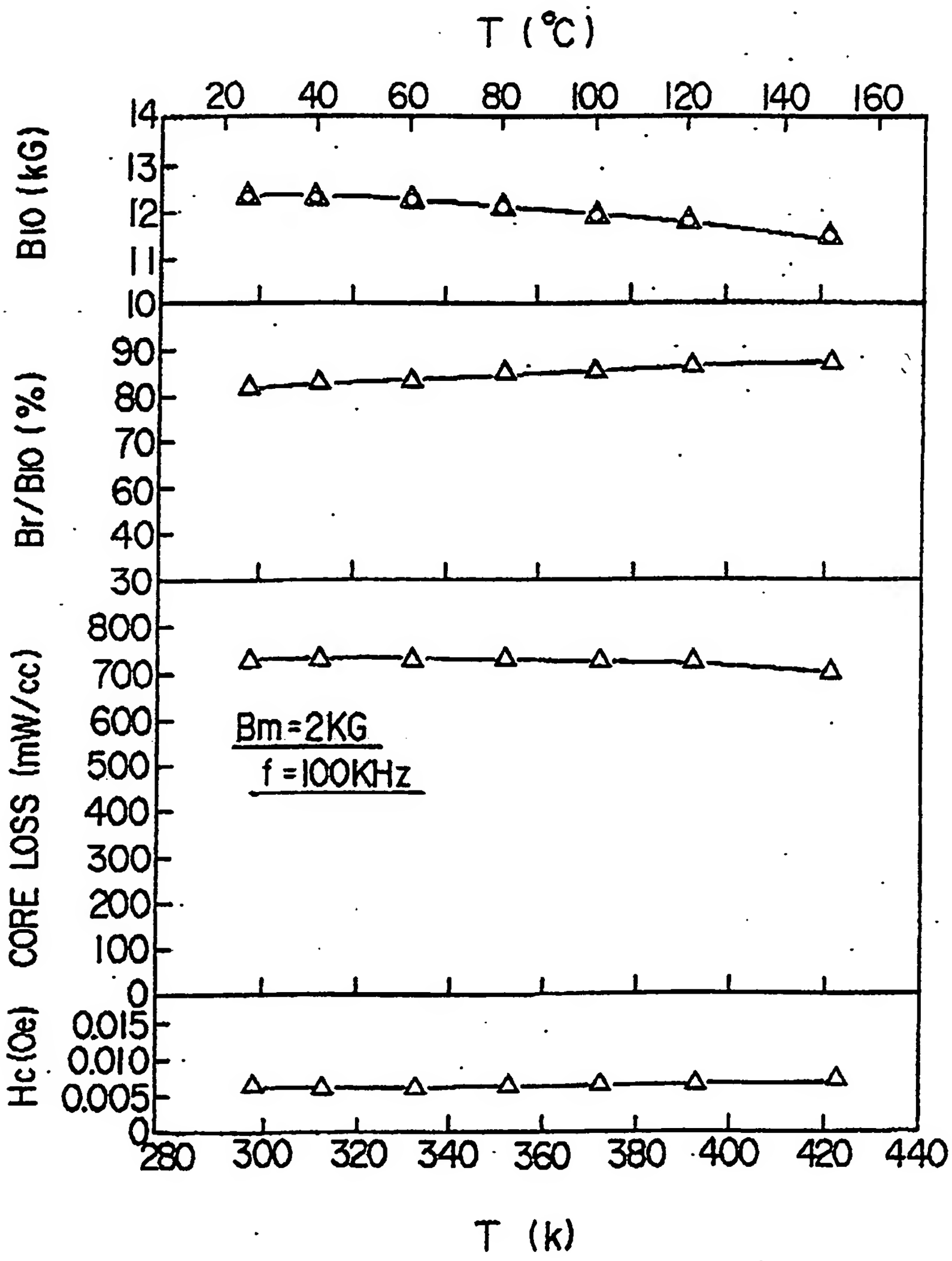
T (°C)
20
40
60
80
100
120
140
160
Bio (kG)
14
13
12
11
10
Br/Bio (%)
90
80
70
60
40
30
CORE LOSS (mW/cc)
800
700
600
500
400
300
200
100
0
Bm=2KG
f=100KHz
Hc (Oe)
0.015
0.010
0.005
0
280
300
320
340
360
380
400
420
440
T (k)

FIG. 12

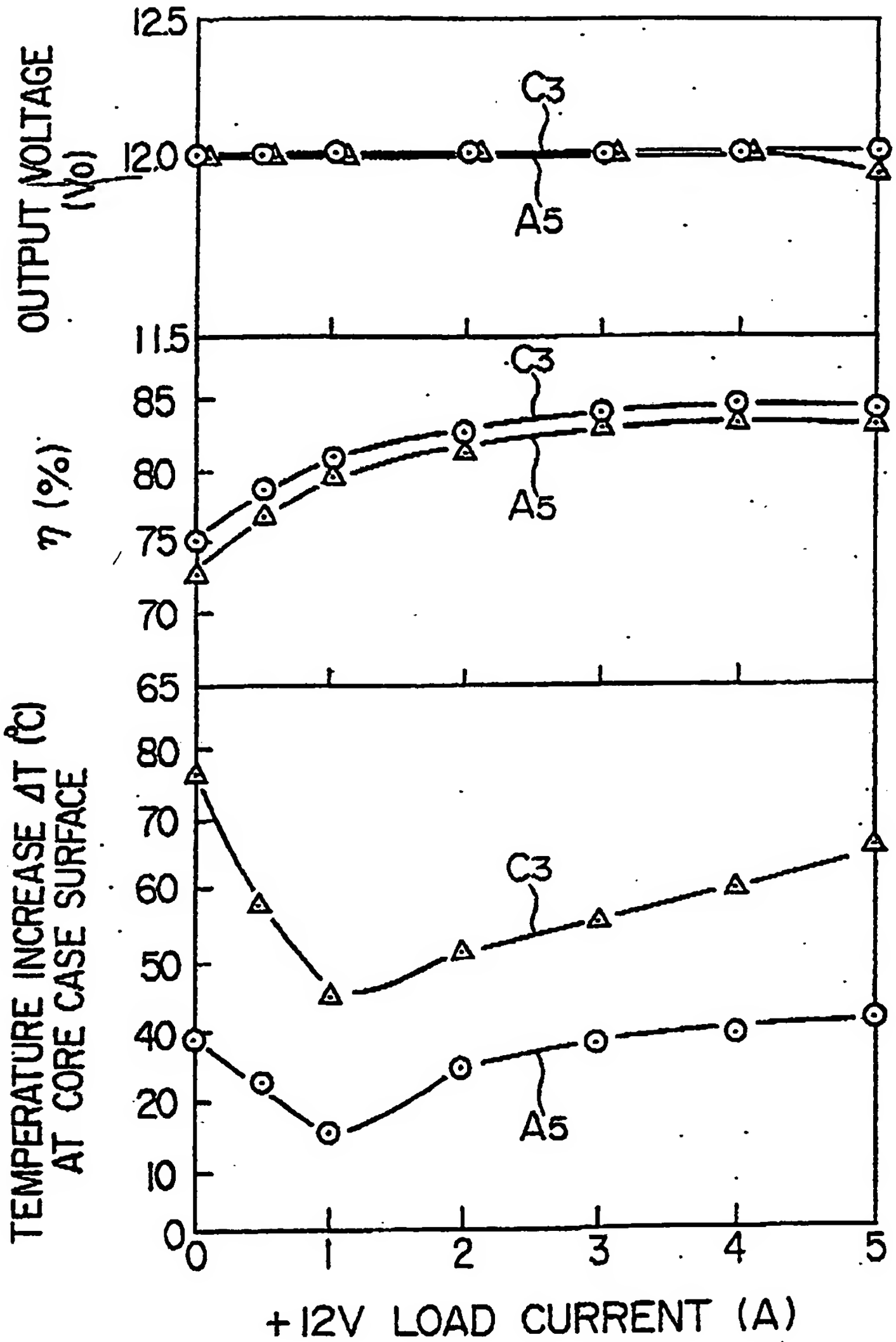
OUTPUT VOLTAGE (Vo)
12.5
12.0
11.5
C3
A5
η (%)
85
80
75
70
65
TEMPERATURE INCREASE ΔT (°C) AT CORE CASE SURFACE
80
70
60
50
40
20
10
0
0
1
2
3
4
5
+12V LOAD CURRENT (A)

FIG. 13

(a)

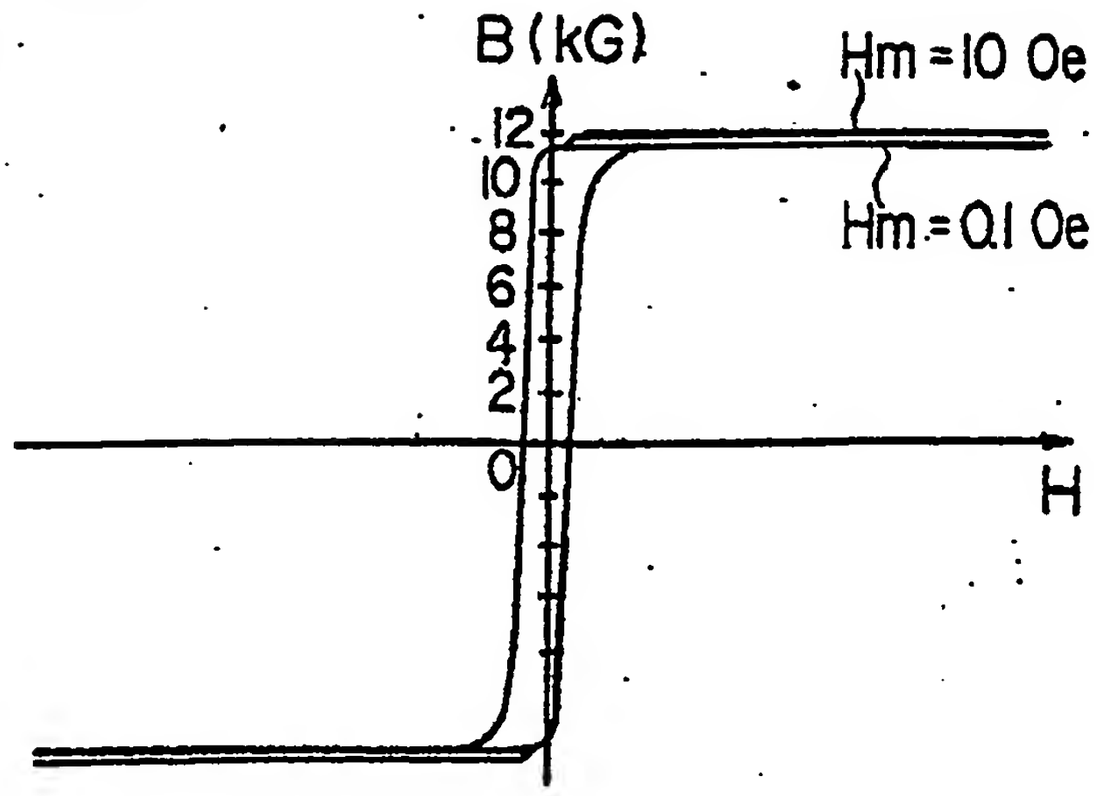
B (kG)
Hm = 10 Oe
Hm = 0.1 Oe
12
10
8
6
4
2
0
H

(b)

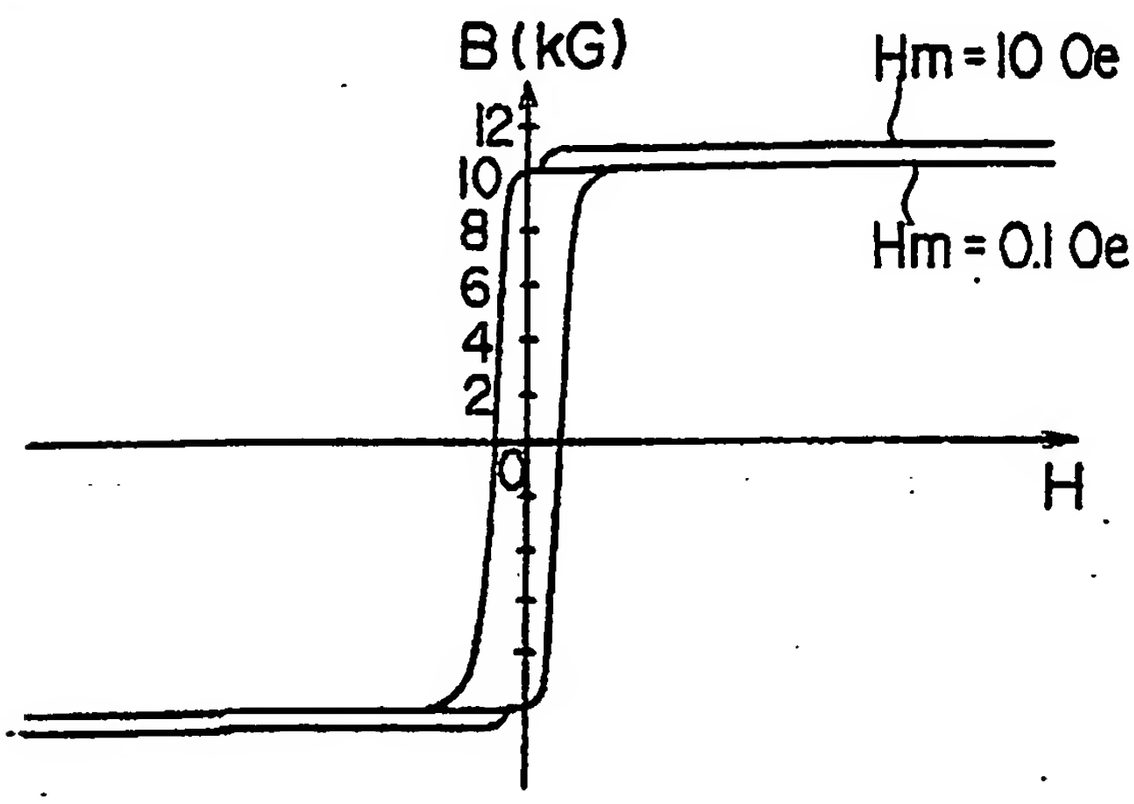
B (kG)
Hm = 10 Oe
Hm = 0.1 Oe
12
10
8
6
4
2
0
H

(c)

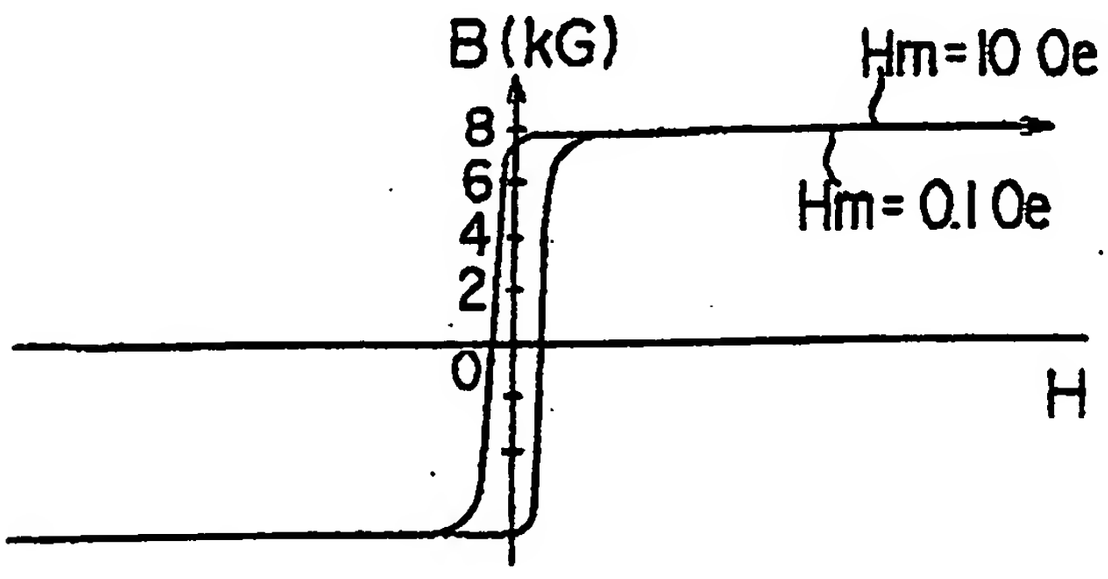
B (kG)
Hm = 10 Oe
Hm = 0.1 Oe
8
6
4
2
0
H

FIG. 14

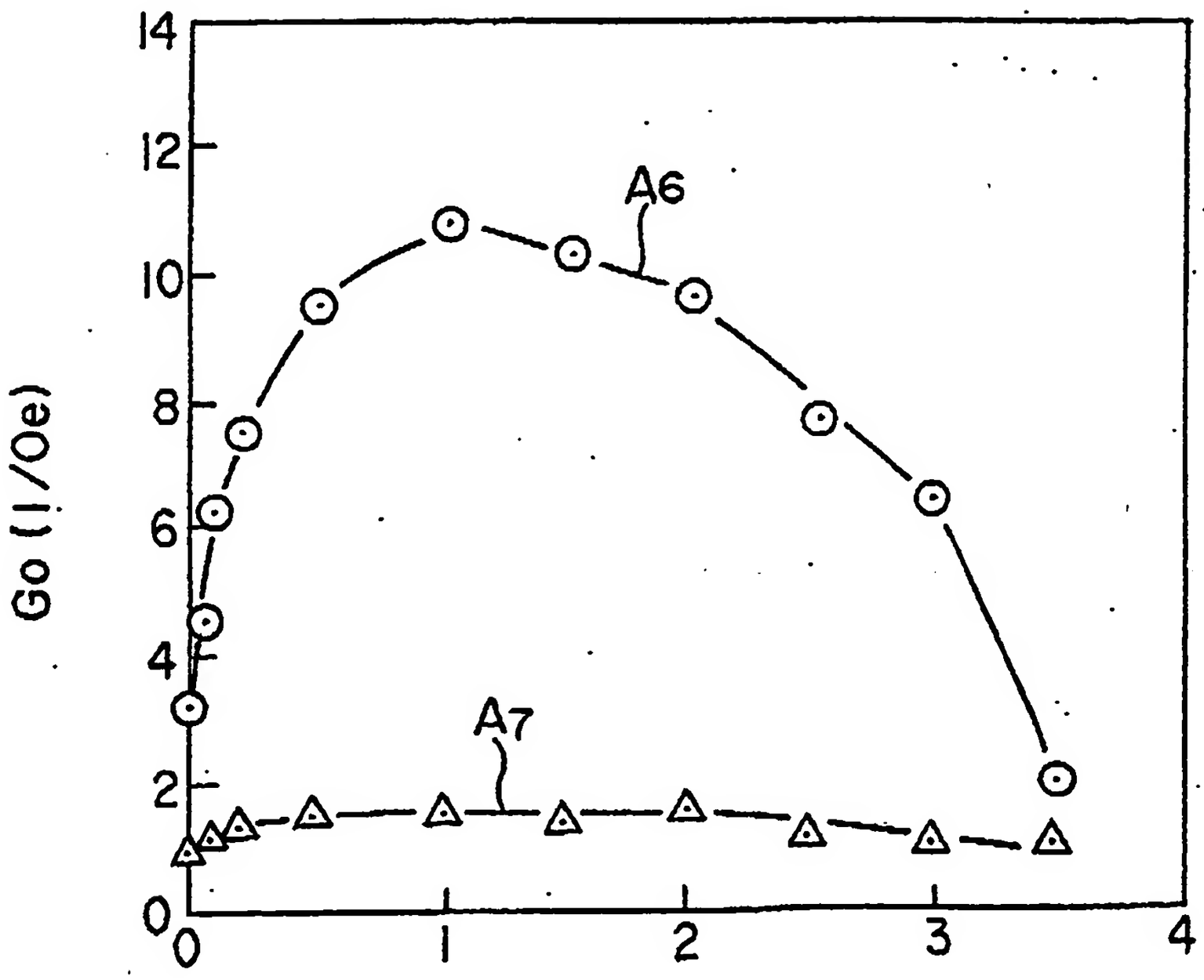

FIG. 15

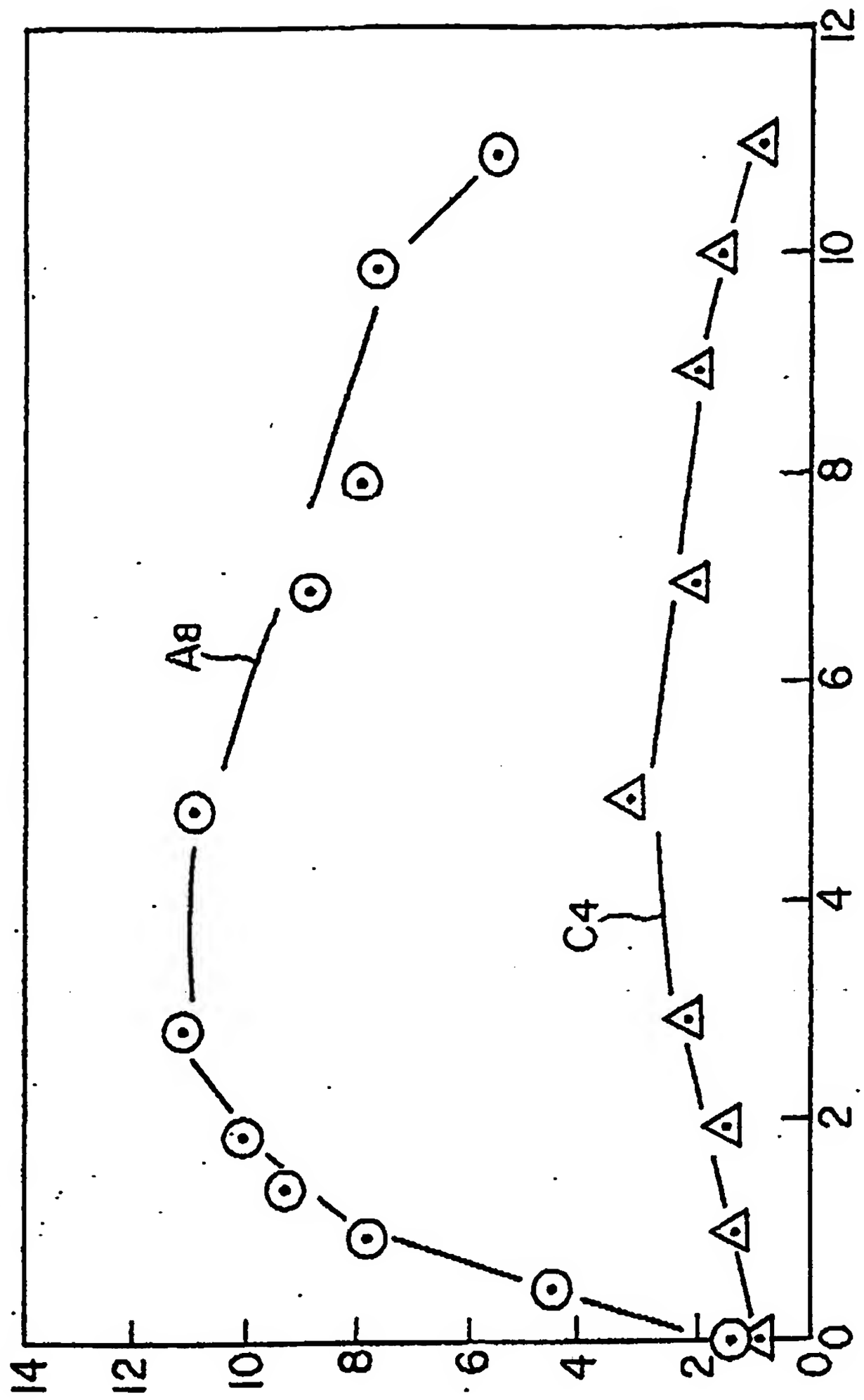

FIG. 16

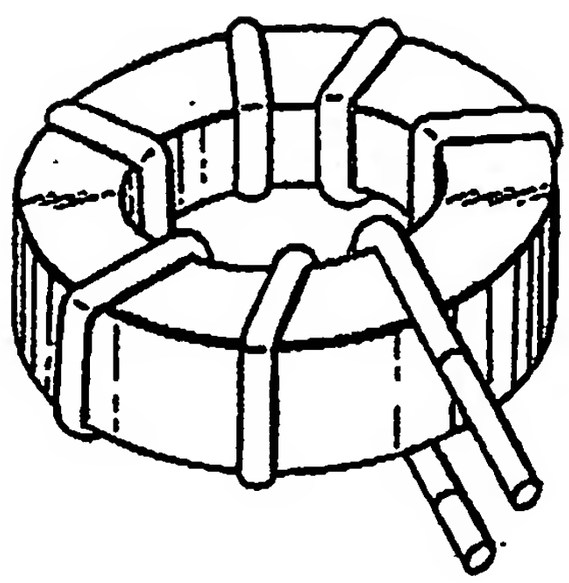

FIG. 17

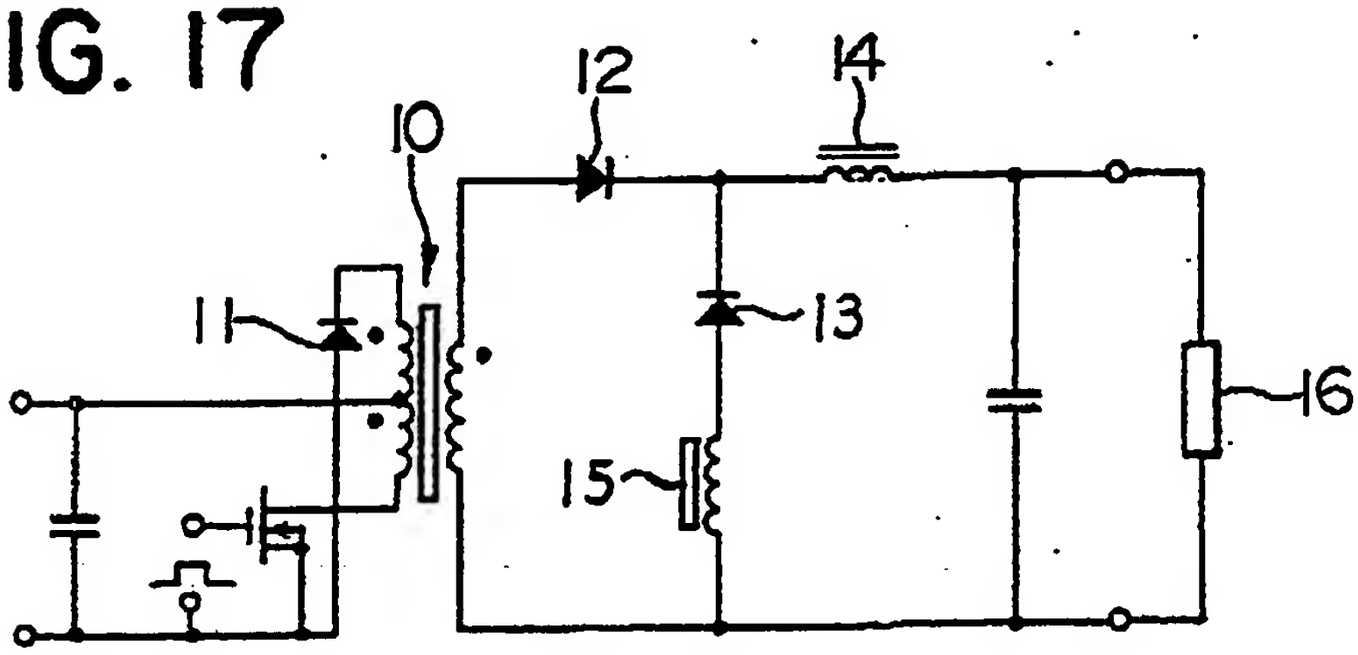

FIG. 18

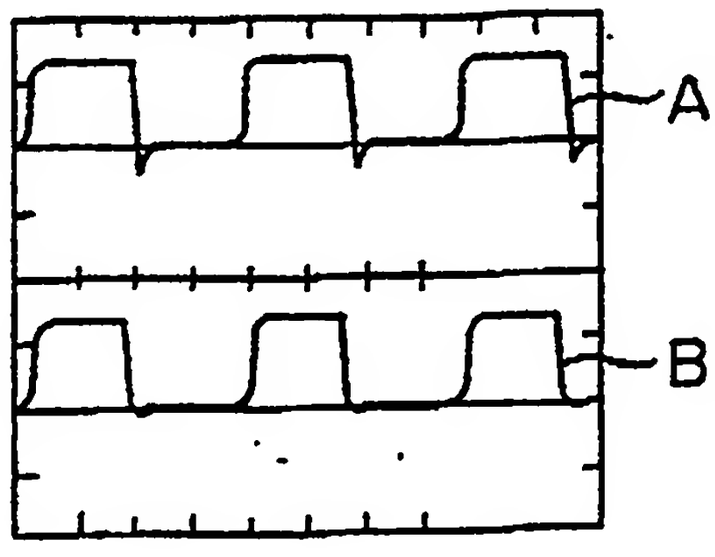

FIG. 19

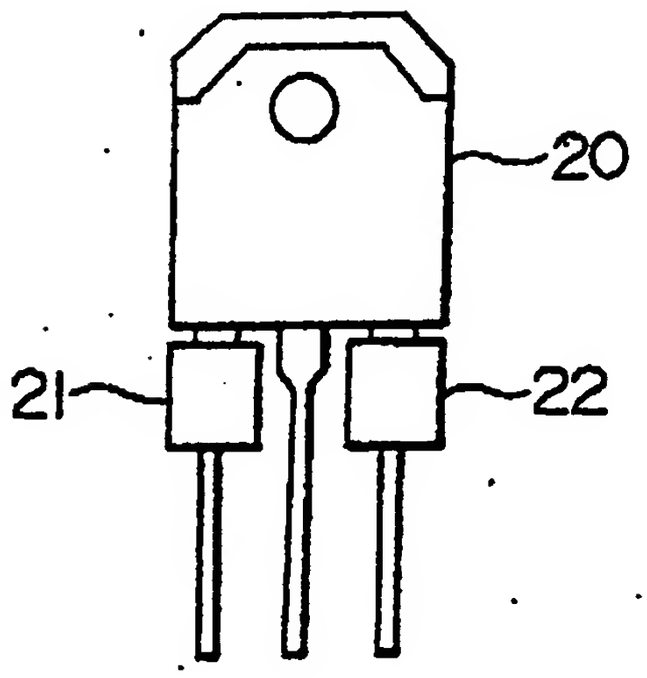

FIG. 20

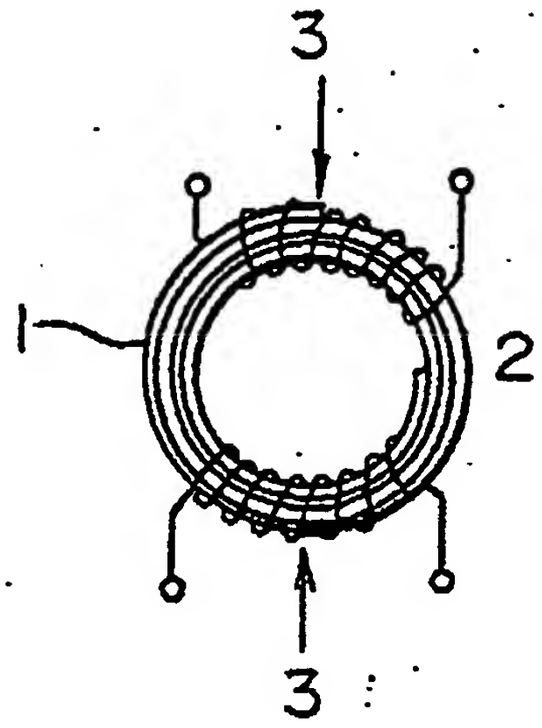

FIG. 22

(a)

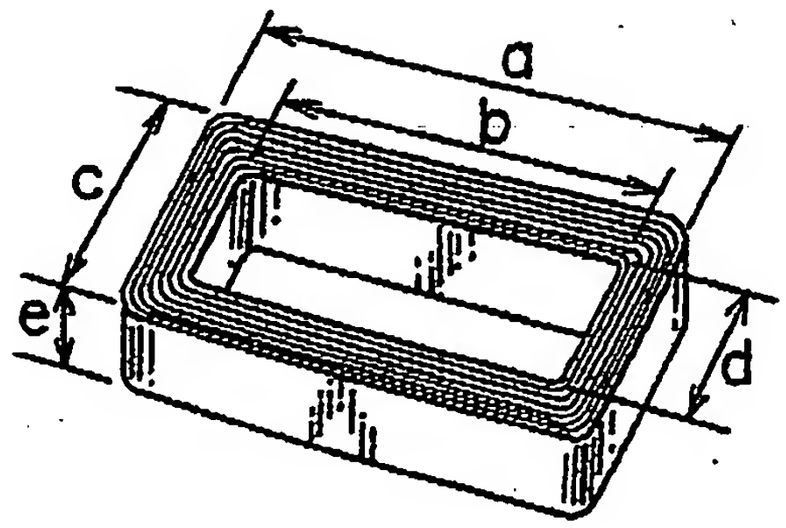

(b)

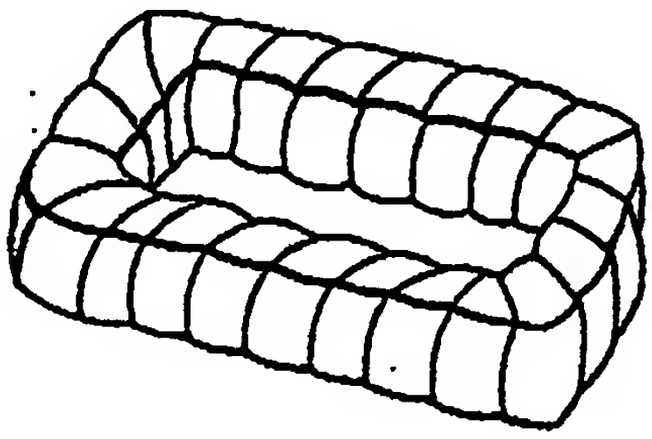

FIG. 21

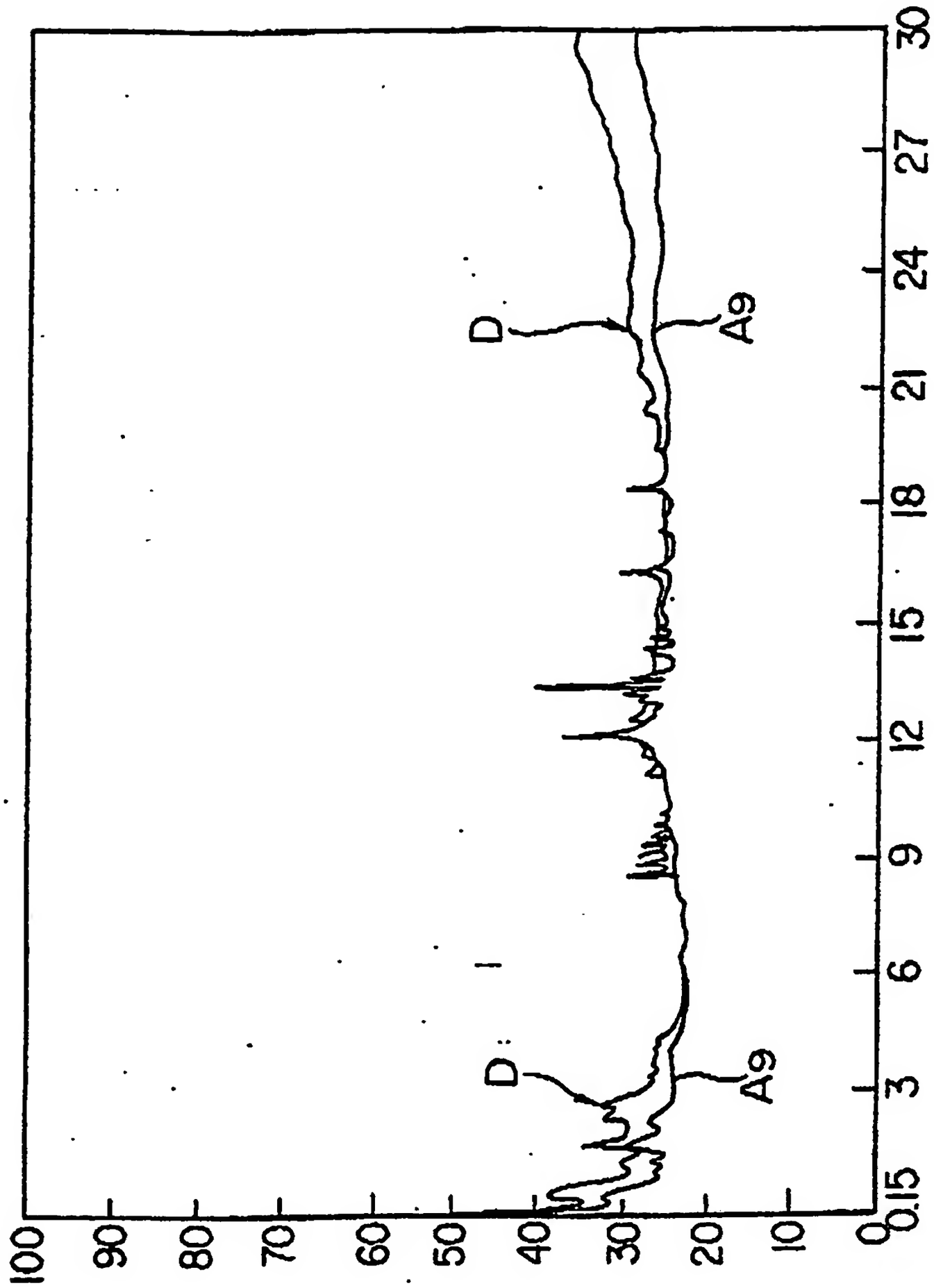
D
A9
D
A9
30
27
24
21
18
15
12
9
6
3
0.15
f (MHz)
100
90
80
70
60
50
40
30
20
10
0
NOISE LEVEL (dBμV)

FIG. 23(a)

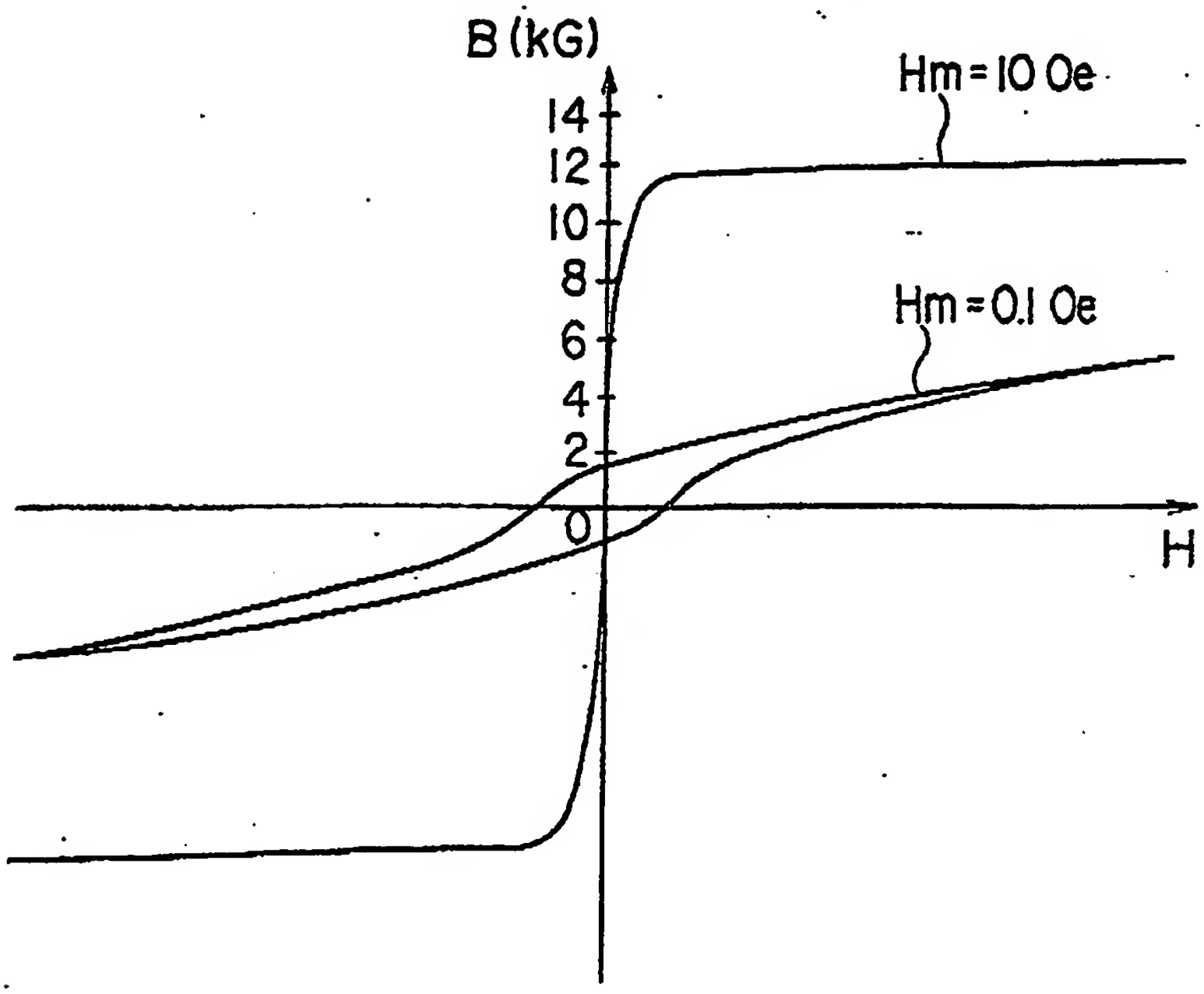

FIG. 23(b)

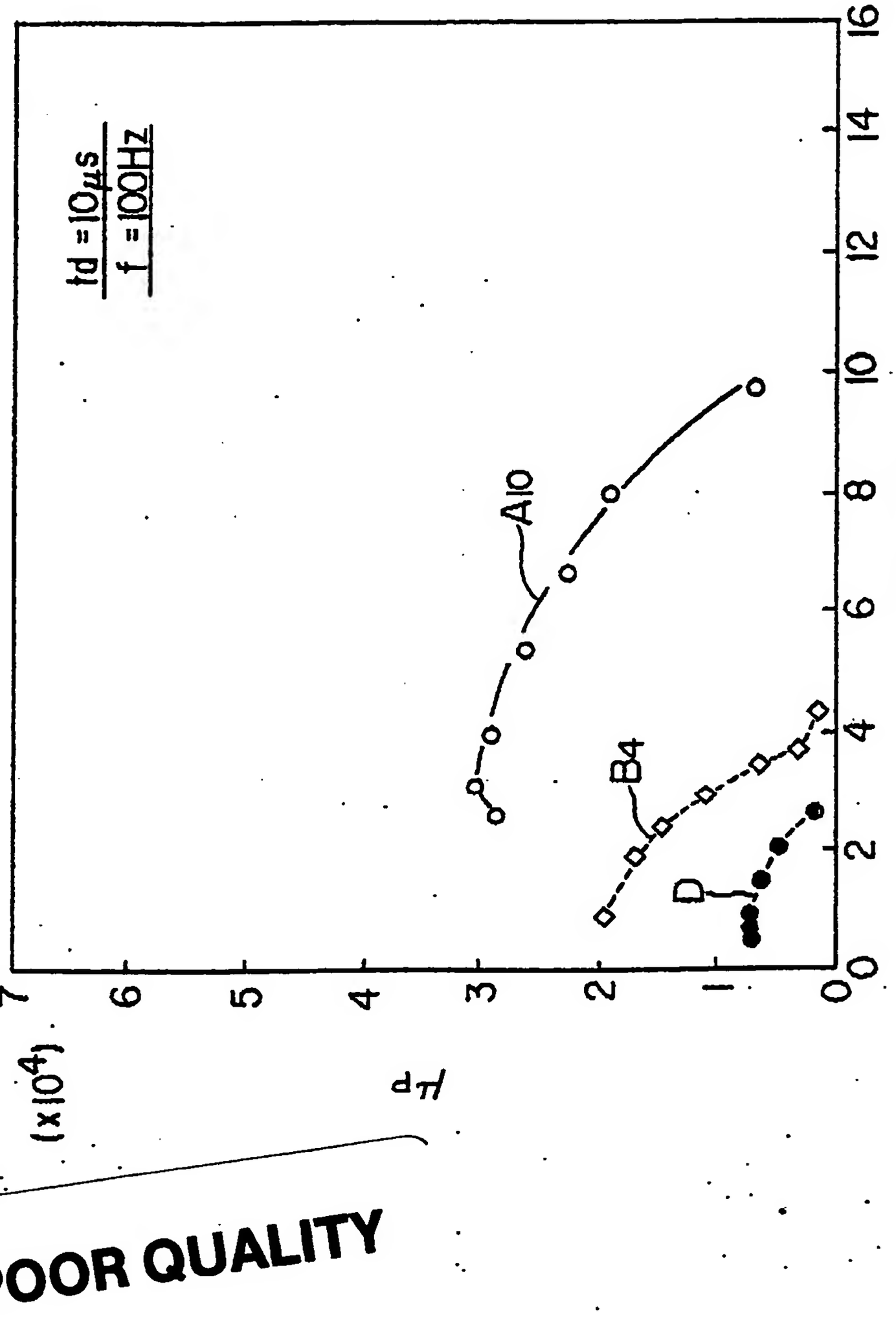

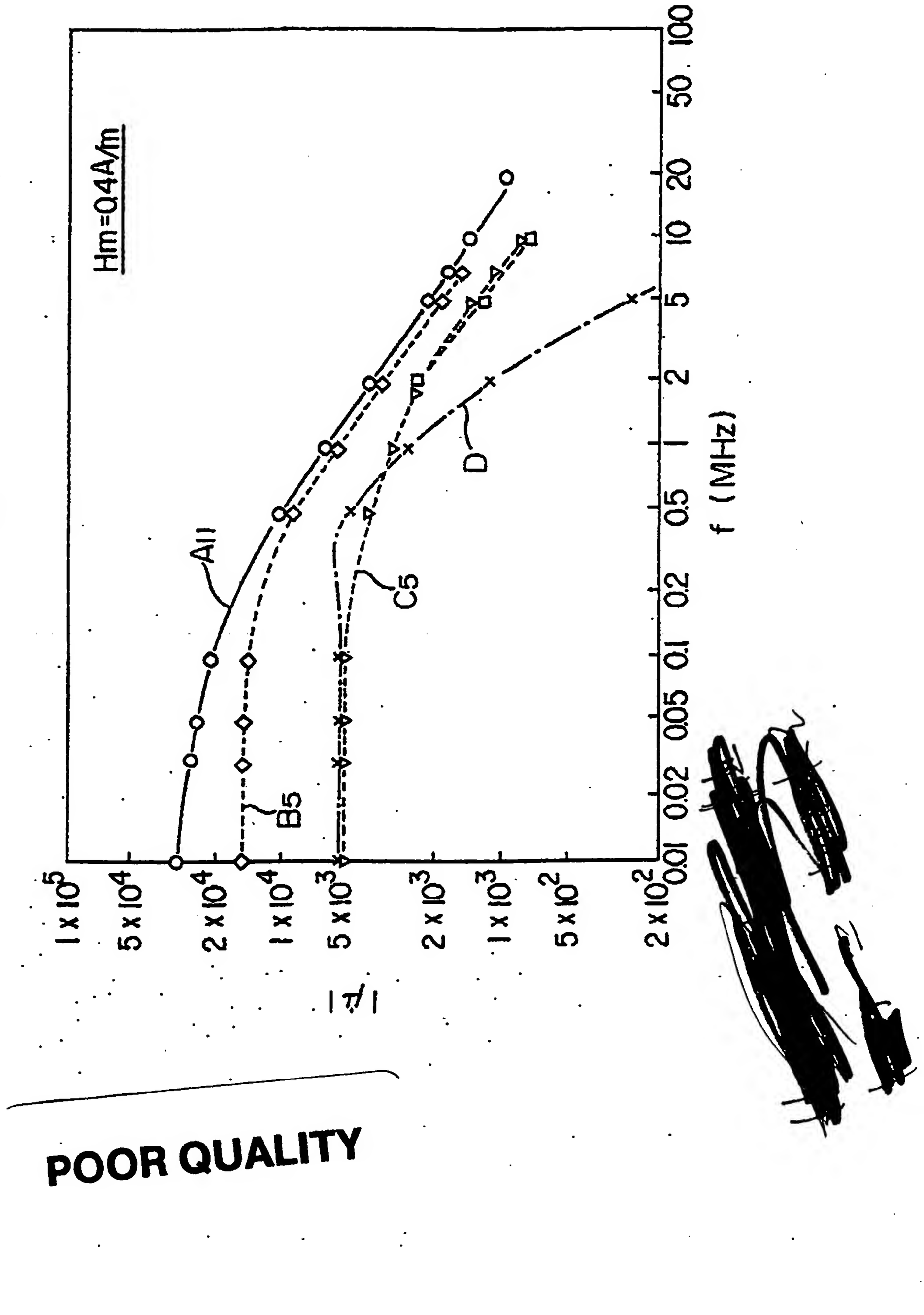

FIG. 24

FIG. 25

(a)

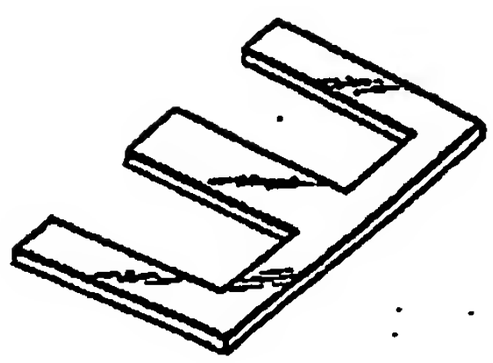

(b)

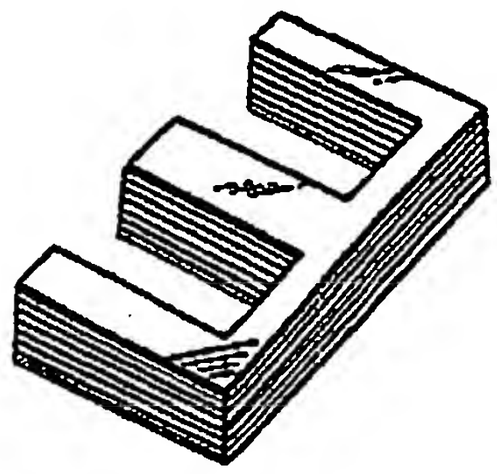

FIG. 28

(a)

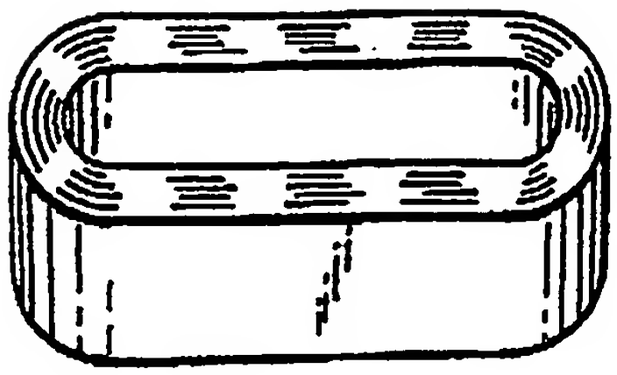

(b)

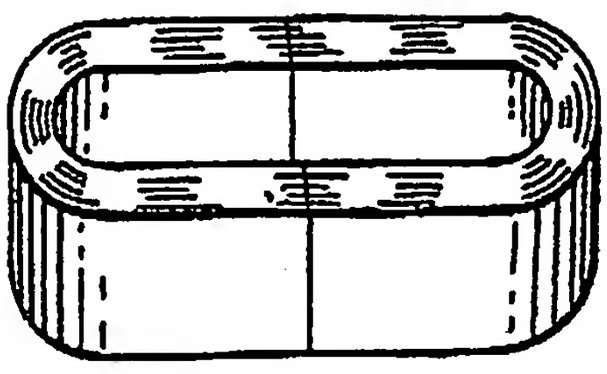

FIG. 26 (a)

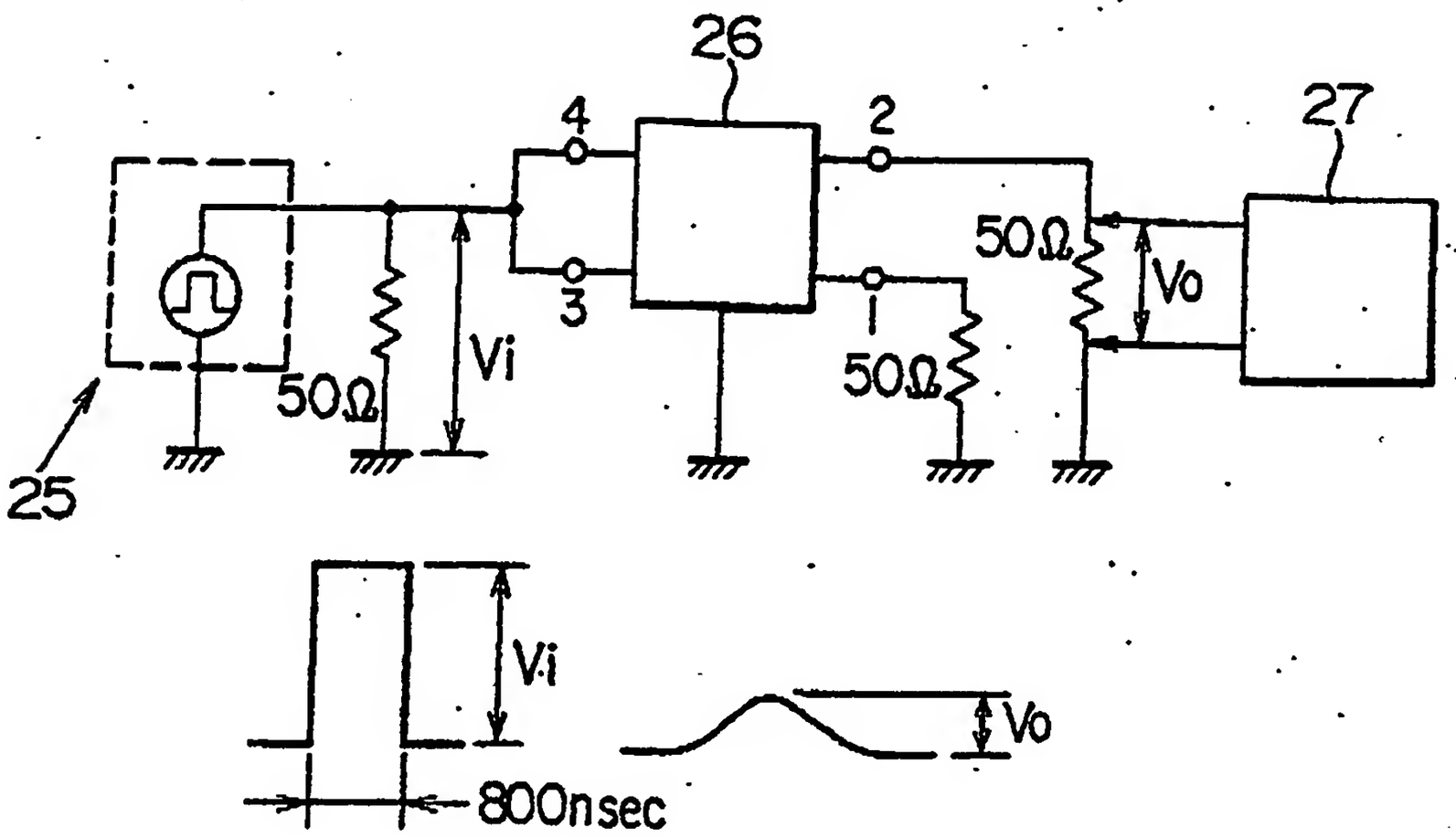

FIG. 27 (a)

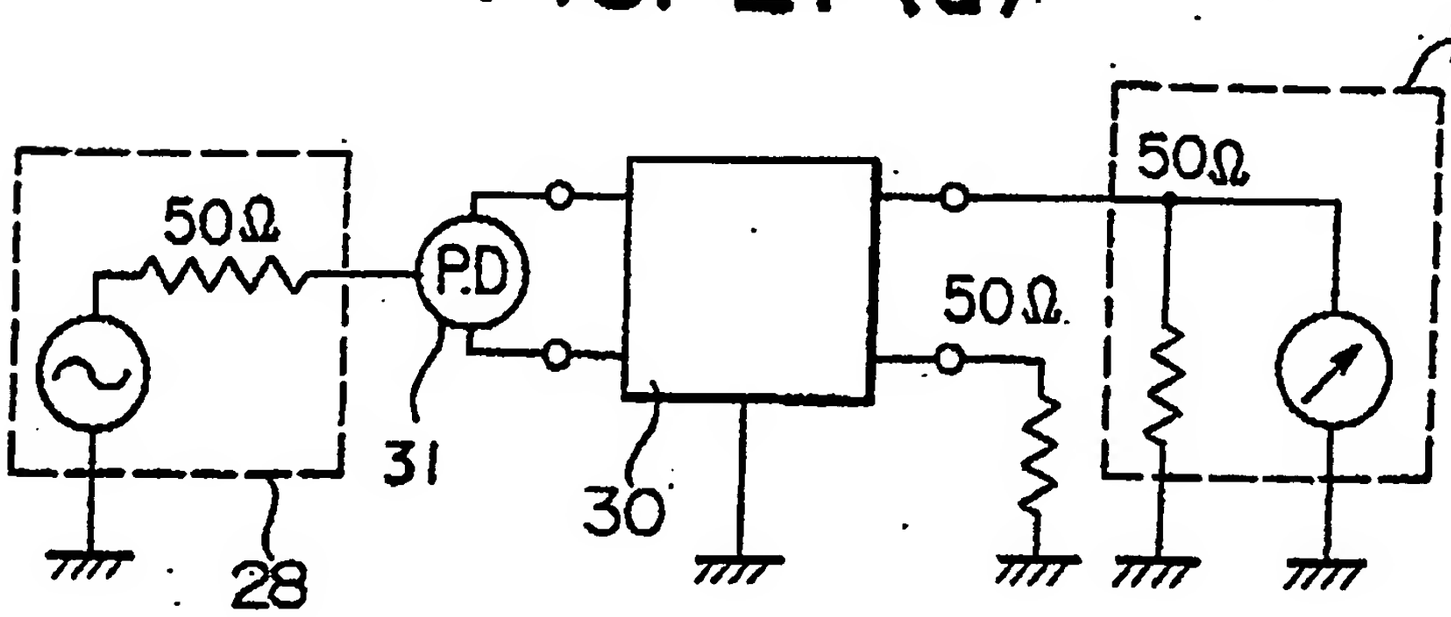

FIG. 26(b)

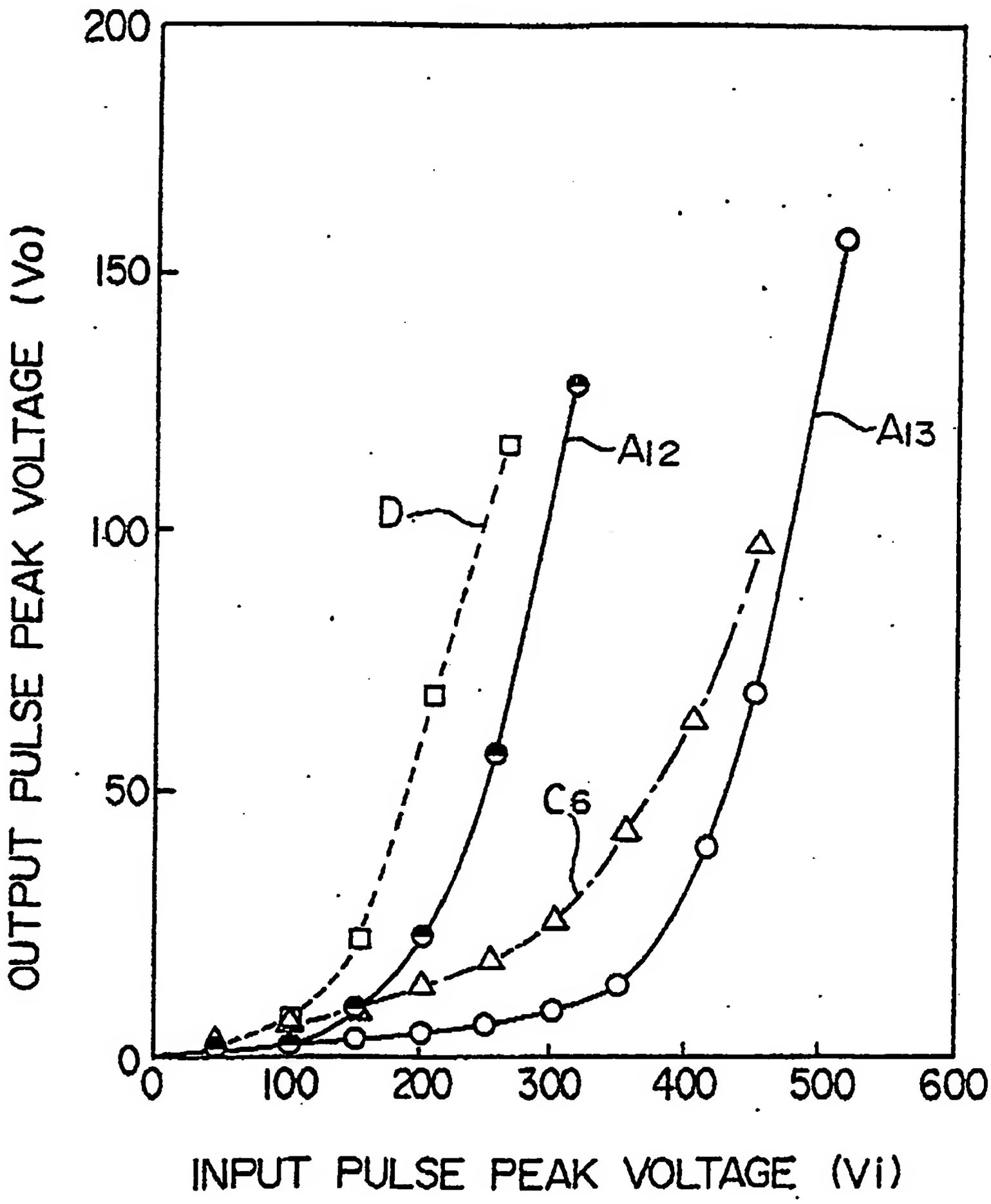
200
150
100
50
0
0
100
200
300
400
500
600
OUTPUT PULSE PEAK VOLTAGE (Vo)
INPUT PULSE PEAK VOLTAGE (Vi)
D
A12
A13
C6

FIG. 27 (b)

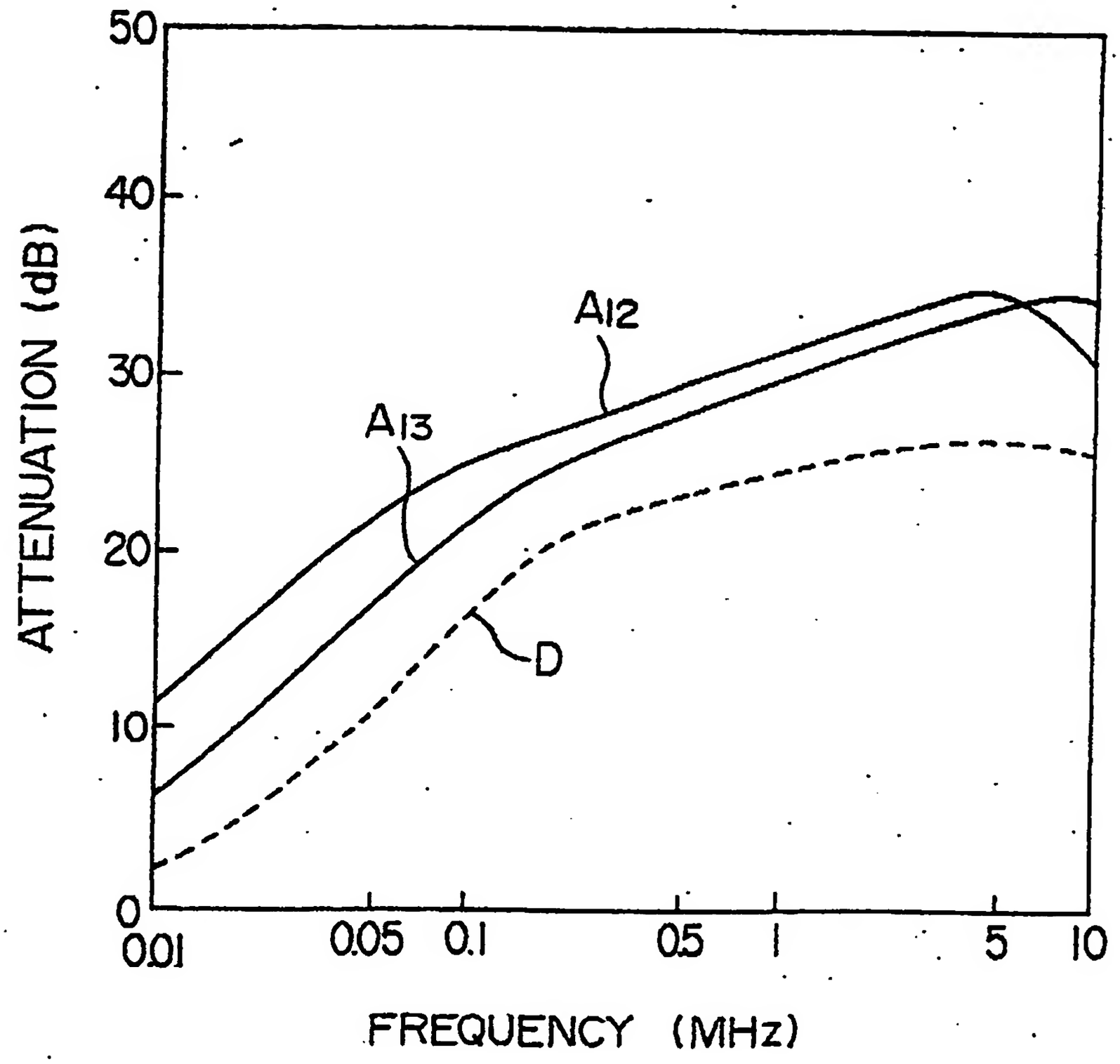
50
40
30
20
10
0
ATTENUATION (dB)
A12
A13
D
0.01
0.05
0.1
0.5
1
5
10
FREQUENCY (MHz)

FIG. 29

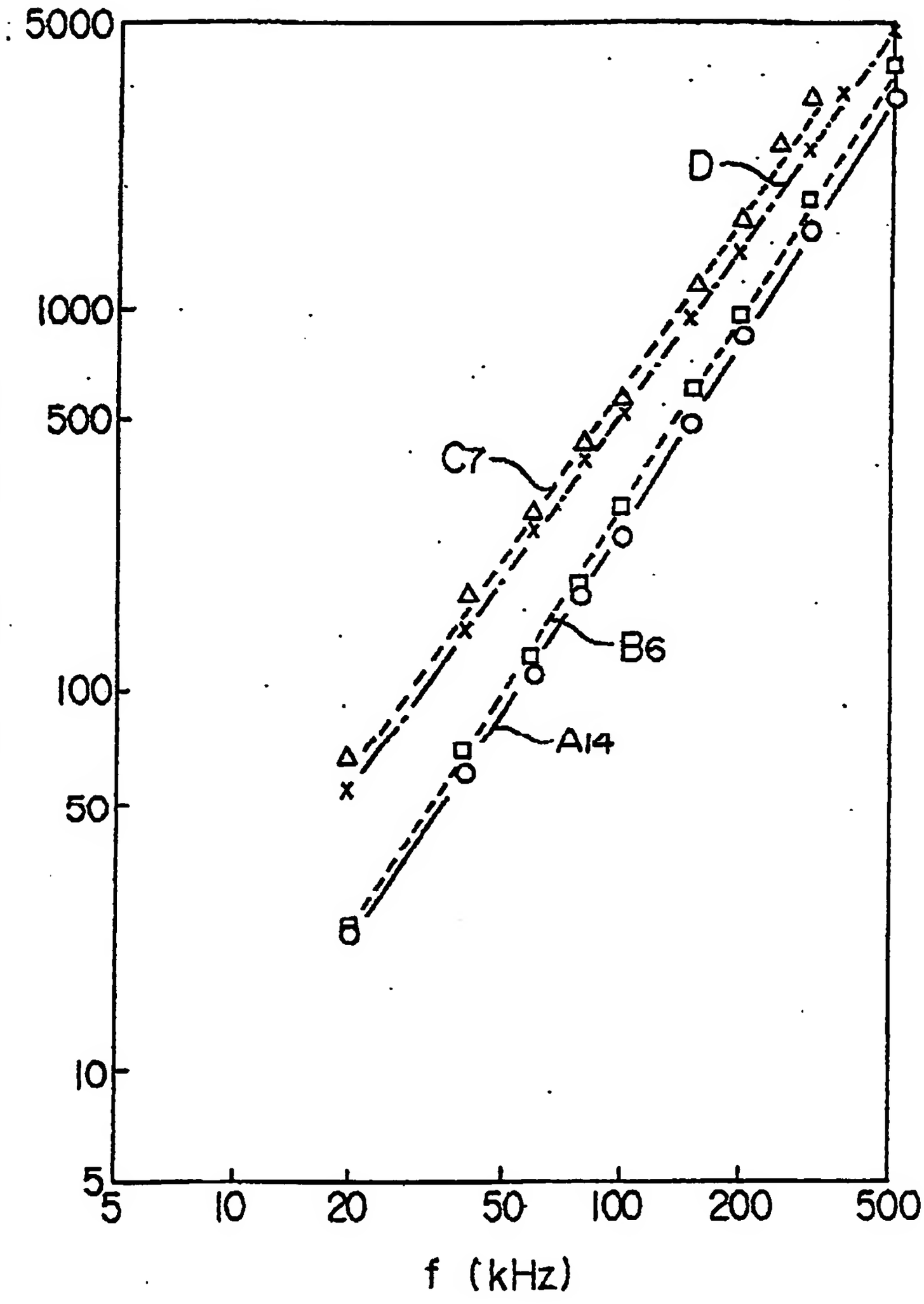
5000
1000
500
100
50
10
5
CORE LOSS (mW/cc)
D
C7
B6
A14
B
5
10
20
50
100
200
500
f (kHz)

European Patent Office

EUROPEAN SEARCH REPORT

. Application number

EP 88111364.1

DOCUMENTS CONSIDERED TO BE RELEVANT

Category	Citation of document with indication, where appropriate, of relevant passages	Relevant to claim	CLASSIFICATION OF THE APPLICATION (Int. Cl.4)
A	US - A - 4 558 297 (SHIGETA) * Abstract; claims 1-13 * --	1,13	H 01 F 27/24
A	GB - A - 2 102 212 (TELCOR) * Abstract; claims 1-7 * ----	1,13	

TECHNICAL FIELDS SEARCHED (Int. Cl.4)

H 01 F 27/00
H 01 F 1/00
H 01 F 19/00

The present search report has been drawn up for all claims

Place of search	Date of completion of the search	Examiner
VIENNA	17-10-1988	VAKIL

CATEGORY OF CITED DOCUMENTS

X : particularly relevant if taken alone
Y : particularly relevant if combined with another document of the same category
A : technological background
O : non-written disclosure
P : intermediate document

T : theory or principle underlying the invention
E : earlier patent document, but published on, or after the filing date
D : document cited in the application
L : document cited for other reasons

& : member of the same patent family, corresponding document

EPO Form 1503. 03.82